PROCESS CALIBRATION FOR ELASTICALLY SCALED 3D PRINTED MODELS USING FUSED DEPOSITION MODELING

By

Edgar Bernardo Mares

Presented to the Faculty of the Graduate School of

The University of Texas at Arlington in Partial Fulfillment

Of the Requirements

For the Degree of

MASTER OF SCIENCE IN MECHANICAL ENGINEERING

THE UNIVERSITY OF TEXAS AT ARLINGTON

December 2018

Acknowledgements

I would like to express my gratitude to my supervising professor Dr. Robert Taylor for helping me throughout the development of my work. He has guided me and was one of the few professors that motivated me to pursue my masters in mechanical engineering. I would not be here if it was not for the constant encouragement he has provide me.

I would also like to thank my thesis defense committee, Dr. Ashfaq Adnan and Dr. Endel Iarve for their comments and time. Their expertise and knowledge was a learning experience. Lastly I want to give a special thanks to my family for supporting me and keeping me motivated throughout my entire education.

Abstract

PROCESS CALIBRATION FOR ELASTICALLY SCALED 3D PRINTED MODELS USING FUSED DEPOSITION MODELING

Edgar Bernardo Mares, MS in Mechanical Engineering

The University of Texas at Arlington

Supervising Professor: Dr. Robert Taylor

With the increase in additive manufacturing capabilities the use of 3D printed models characterize a critical point for evaluating aerodynamic and aeroelastic properties on aircraft configuration. An experimental and computational approach beginning with elastically scaled 3D printed models enables for a case to be defined, developed, and extracted to match aeroelastic test behavior. The basis of this work is supported by aeroelastic tailoring and scaling methods in the application of 3D printed models. To accomplish this, stiffened 3D printed plates are scaled from elastically scaled 3D printed models for stiffness through geometric configurations, different build orientations, and bead thickness as the driving factors. The methodology developed in this case study shows that build orientation has a considerable effect on stiffness but, not as significant as build configuration and bead thickness. This is seen throughout all 3D printed plates that were printed along the ZX axis 0^0 orientation instead of the ZX axis 45^0 orientation. However, the 3D printed models with the 45^0 configurations had a significant decrease in stiffness when printed at a 45^0 orientation. This means printing in the ZX axis with zero orientation results in the highest overall stiffness. The methodology is presented such that stiffness tuning and tailoring can be calibrated for variations in the design.

Table of Contents

List of Figures

List of Tables

Chapter 1

Introduction

With the advancement in additive manufacturing scaled wind tunnel models of aircraft configurations are used to simulate aerodynamic and aeroelastic behavior of an aircraft. Resulting in quicker and lower cost development for these models. In assessing aerodynamic configurations models can be 3D printed with a high enough thickness that deformation is not a huge factor. This high stiffness in a model is ideal for aerodynamic configurations but for correlating the aeroelasticity of the model to the aircraft it needs to be scaled properly and correctly as it is a very significant factor. Conventional aeroelastic wind tunnel models consists and require multiple individual parts that are fabricated separately. Manufacturing these parts and assembling them to a scaled stiffness is a main contributor of time and build costs. In 3D printed models the idea is to design a configuration that scales stiffness to geometry and material by making it a single piece. By having all of the parts combined and configured into a single part it can help with keeping fabrication cost down as well as overall time. However, in the field of additive manufacturing the process and the material are factors that affect how parts perform.

Additive manufacturing has limitations that are due to the inherent nature of polymer materials. Furthermore, the extent of these limitations varies with 3D printing processes and can relatively influence aeroelastic performance. These kind of limitations play a huge portion on how an aeroelastic model must be engineered. Stiffness being a big factor for aeroelastic behavior is affected by the material due to the discontinuities, defects and bond strength during the layering process of the model. Since thermoplastic polymers are highly dependent of the build direction and layering, certain 3D printing technologies have significantly different mechanical properties. These discrepancies are commonly seen in vertical builds or builds

involving the z-direction. In order for an aeroelastic model to take advantage of the time and cost saved from these 3D printing technologies the model must be properly designed for these material properties and limitations.

The focus of this work is to develop a process for elastically scaled 3D printed models and properly validate this methodology. The methodology proposed is to first take an experimental approach testing scaled 3D printed plates of a full elastically scale wing model. Two different configurations of scaled 3D printed models and two build orientations were tested. The 3D printed plates were tested under two main cases: cantilever beam configuration and a three point bend test. These tests will determine the modulus of the models compared to the stated mechanical properties as well as determine how the model will perform. Additionally, this approach needs to be validated and justified.

Once the tests were concluded and the results interpreted, a computational approach utilizing finite element analysis needs to be made to correlate both results. Creating an accurate finite element model requires that the conditions placed on the model to be exactly as during the experimental stage. Altair HyperWorks, a computer-aided engineering program will be used to create a finite element model. Allowing for finite element analysis to be performed on the model and then compared back to the original experimental tests.

The need to calibrate and test these 3D printed plates play a significant portion in comparing real world results to a bounded simulated program. Ultimately the ideal goal of the methodology is to tune and tailor aeroelastic behavior of the 3D printed model until achieving the desired performance.

Chapter 2

Background

Research on additive manufacturing and aeroelasticity and its variants were conducted to develop a background. The background is comprised of published articles, documented information, published book and online references. Building up a data base of knowledges is crucial to the study of this project, as this provides the base information needed in order to develop a methodology.

2.1 Additive Manufacturing

The basic idea of additive manufacturing (AM) is to add layers of material unlike conventional manufacturing that relies on taking away from a component. Additive manufacturing brings a digital flexibility and efficiency that prior manufacturing lacks. This new type of flexibility allows for more complex and organic geometries to be constructed. In traditional methods machines are limited by the tools available. Where distinct processes for each job and part needs to be done at different machines. Limiting the capability to design complex and internal features. Unlike conventional means additive manufacturing has the ability to rapidly build without the added hassle of having to heavily rely on post processing process.

In the beginning the applications of additive were limited and were not favored when compared to conventional manufacturing. At most it was used for quick modeling and rapid prototyping. The term additive manufacturing is formalized from the previous term rapid prototyping. Where rapid prototyping is described as a process for rapidly creating a system or part representation before final release or commercialization[1]. Improving on the idea of simply creating models additive manufacturing developed over time. More recently, newer technologies

have widen the range of application of these processes and have outputted products suitable for commercial use.

The generic additive manufacturing process follows a series of steps that converts a computer-aided design (CAD) into a physical object. These steps may vary in degrees depending on the product being constructed but the basis of the steps are still present. The generic additive manufacturing steps are listed as follows

1. Create a CAD model
2. Convert CAD model to STL
3. Transfer and manipulate STL for AM machine
4. Machine setup
5. Creation of parts
6. Removal of parts from AM machine
7. Post-processing
8. Application

The benefit of innovating quickly and constantly iterating on those designs is the main appeal of 3D printing.

There are a variety of additive manufacturing processes such as vat photopolymerization, powder bed fusion, fused deposition modeling, sheet lamination, binder jetting, and directed energy deposition. Each with their advantages and disadvantages.

2.1.1 Fused Deposition Modeling

When talking about 3D printing people consider extrusion the most pronounced out of the additive processes. Fused deposition modeling (FDM) is the most common extrusion process

and was developed by Stratasys. It utilizes a heating chamber to liquefy polymer that is fed into the system as filament[1]. The filament is then pushed into the chamber by a tractor wheel arrangement and it is this pushing that generates the extrusion pressure[1]. This extruder nozzle than places thin cross sectional layers on the base plate and stacks them on top of each other until it matches the original CAD model. An example of the extruder is shown in Figure 2-1.

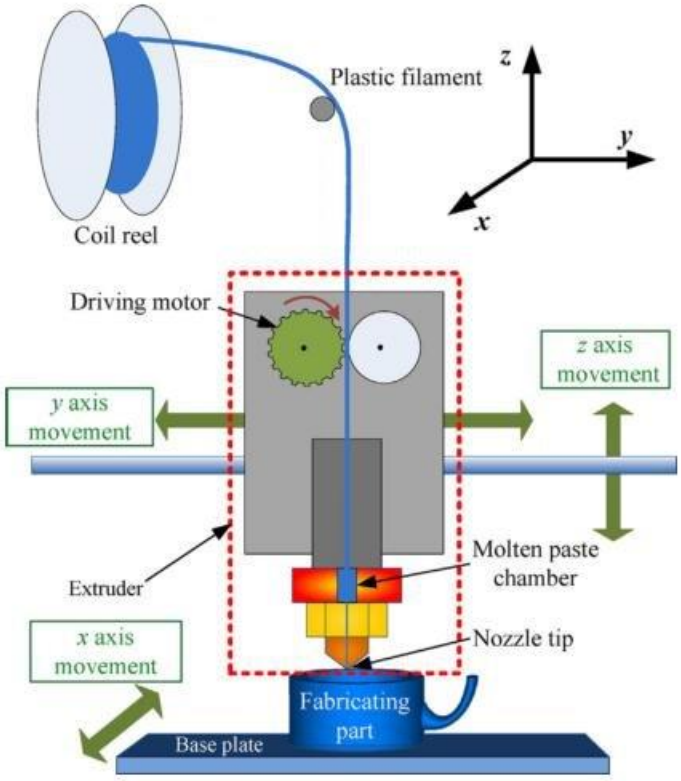

Figure 2-1 Extruder[2]

Fused deposition modeling is like any other additive process in regard to having both pros and cons. One of the advantages to utilizing this process is the wide range of materials that are available. In particular, amorphous polymers like ABS and PLA are best suited for this process because they extrude in a viscous paste rather than in a lower viscosity form. Being this material it means that there is no distinct melting temperature, and the material increasingly

softens and viscosity lowers with increasing temperature[1]. As this material is extruded, the viscosity is high enough that their shape is maintained after extrusion enabling to easily bond with adjacent layers. The effective mechanical properties that result from the extrusion make this the ideal material. These materials must also follow certified industrial standards set by the FDA and FAA.

While these properties are similar to commonly used materials, it should be noted that parts made using fused deposition modeling might exhibit regions of lower strength due to defects, interfacial regions, and voids. The stacking of layers of material on top each other is the cause of this lower strength. For example, as the layers are stacked the bonding between each layer can vary. Causing some areas of the part to be stronger and others weaker. Since layers are stacked in the z direction this is where most problems occur. Keeping the temperature of the extruded polymer consistent is key in having uniform strength throughout the part.

Along with advantages come limitations for the process. While it may be a well-rounded process there is one main drawback, the build speed. As mentioned earlier the inertia of the plotting heads means that the maximum speed and accelerations that can be obtained are somewhat smaller than other conventional systems[1]. Coupled with the need to have the material plotted results in a drawn-out process. Not only is build speed a major drawback but also the size of the machines; more specifically the build volume. The largest being the Objet1000[3], which has a build tray of 1000 x 800 x 500 mm, created by Stratasys.

2.2 Aeroelastic Scaling

The aeroelastic scaling of a wind tunnel model is driven by the characteristics of a full scale aircraft. Scaling a wind tunnel model requires that the model have geometric similarity and

stiffness. For geometric similarity the shape of the model is defined by the geometric parameters of the aircraft. Similarly, the stiffness similarity is defined by the torsional and bending stiffness ratios EI and GJ. By matching flexural stiffness and torsional stiffness a scaled model behaves identically to a full scale aircraft[4].

Flexural stiffness ratio ($EI_{model}/EI_{aircraft}$) for the scaled model is determined by the dynamic pressure scale ($q_{model}/q_{aircraft}$) and the length scale factor ($s_{model}/s_{aircraft}$). In the case for a static aeroelastic scaling, the length scale factor is determined by the wind tunnel test section. The same procedure can be done to scale the torsional stiffness ratio ($GJ_{model}/GJ_{aircraft}$).

2.3 Aeroelastic Tailoring

As defined by Shirk, et al[5], "Aeroelastic tailoring is the embodiment of directional stiffness into an aircraft structural design to control aeroelastic deformation, static or dynamic, in such a fashion as to affect the aerodynamic and structural performance of that aircraft in a beneficial way". Aeroelastic tailoring is not a completely new concept. The development of this theory has been applied plenty of research studies. Aeroelastic tailoring has provided the means of expanding design. The directional stiffness properties in composites achieved by stacking layers in a specific order is an example. Additionally, variations in symmetry and stacking of layers can cause coupling between in-plane and out-of-plane deflections. With this type of manipulation designers can design for bend-twist coupling and bend-camber coupling. For example, on an aircraft wing there are two specific designs affected by tailoring. In the first design it is called wash-in. In this case, the root of the wing is attached at a lower angle to than the tips. During stall the wing tips experience stall first before the root of the wing. Wash-out on the other hand is the opposite. The wing root has a higher angle of attack than the wing tips. In

this design the wing root is what stalls first and is most cases it is the desired design. Having the wing root stall first helps with maintaining control of the aircraft during stall.

2.4 Aeroelasticity in the Context of Additive Manufacturing

Aeroelastic scaling and tailoring for 3D printed wind tunnel models are thriving of the advances in additive manufacturing. With the ability to fabricate parts by depositing materials in uniform layers the more organic and complex the parts can become. Enabling for more cost effective and rapid fabrication for tuning and tailoring stiffness. The aeroelastic tailoring and tuning do not change when designing for additive manufacturing methods. The available methods even allow for the increase in complexity of the model. These types of complexity range from stiffening arrangements, material distribution and even microstructures within the model. All of these parameters affect how stiffness plays a huge role in aeroelastic tailoring and scaling in the model.

When designing wind tunnel models for additive manufacturing only a handful of research has been done on aeroelastic tailoring[6,7]. While the majority of 3D printing methods have been applied to aerodynamic wind tunnel models[8,9,10,11], the methods that work in those applications can also apply for aeroelastic tailoring. Methods such as fused deposition modeling, selective laser sintering, stereolithography, and material jetting are the most common 3D printing technologies used for these models.

The benefit of designing models for additive manufacturing come with their share of constraints and limitations. For aeroelastic tailoring the design can be manipulated to obtain the desired stiffness. This is done by either rearranging the substructure, cross section configuration,

or skin thickness. Once designed properly they can be implemented for fused deposition modeling as shown in Figure 2-2.

Figure 2-2 Examples of Stiffness Tailoring through Additive Manufacturing[12]

The designs in Figure 2-2 show how the complex interior can be designed more freely through additive manufacturing

Additionally, the fabrication limits how the models are tailored. The 3D printing technologies mentioned earlier all have the same kind of process. They convert material into 3D geometry by layering the material in individual layers through continually depositing material along a formulated path. This kind of process and bonding occurring between layers greatly affect the material and geometric capability. The material capability of the models are defined by the voids and gaps that are intrinsic when bonding layers in this method. Consequently, the model is very dependent on the direction of layering making it anisotropic. On another hand, the overhangs and bridging during the fabrication greatly affect stiffness and strength in the model. Each of these constraints must be accounted for in the aforementioned processes. By designing

with the limitations in mind a 3D printable model can be developed and provide an innovative approach for aeroelastic tailoring.

Although the 3D printing technologies all have different strength and weaknesses, there are common characteristics shared by all. The reduction in strength when building is the most common characteristic shared. When building in certain directions the strength of the model can vary drastically. For example, when building in the Z-direction the strength can be significantly lower than in-plane strengths[13]. The gaps and voids during the layering are the main cause why the material does not maintain complete continuity. When utilizing additive manufacturing the mechanical and physical properties will always be lower than that of conventional because of that incomplete cohesion between interfaces. When looking only at fused deposition modeling the reduced strength comes from the slight changes in thermal gradients when the layers are being placed on top of one another. The variation of bonding between layers creates the voids that build up the stress in that region. Ultimately causing catastrophic failure when the stress level is significantly lower than what is predicted.

Along with the strength variation the material discontinuity creates stiffness variation. For example, during fused deposition modeling such variations are just due to the material limitations. In order to keep the mechanical properties closer to bulk polymer properties a few approaches are taken

1. Particle infusion to strengthen and stiffen along bead direction[14]
2. Plasma heating process and CNT coated filament for enhanced interfacial bonding strength[15]
3. Microstructured monofilaments[16]

4. Component post-build heat treatment to increase polymer bonding[17], diffusion, and randomization based on chain dynamics[18,19]

Furthermore, when trying to achieve desirable mechanical properties a tradeoff must be made. Geometric accuracy is lost when trying to obtain better mechanical properties. For example, in fused deposition modeling, when the parameters are changed to incorporate overlap between materials it significantly increases bond strength but consequently when trying to increase bead strength the material spreads over key defining design features. In a thin wall design the structure will change the desired contours. Ultimately developing an undesirable structure.

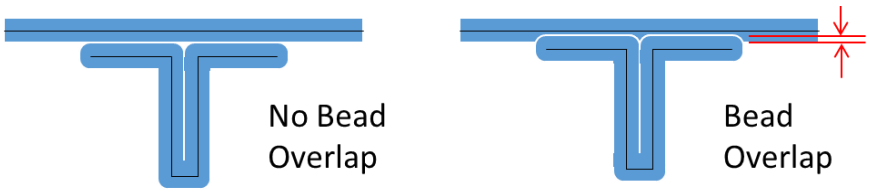

Figure 2-3 Effect of Bead Overlap on Material Continuity

In Figure 2-3, the undesired contour that occurs from the bead overlap that enhances the bond strength can be seen.

Lastly, the bonding of the layers when orientated changes respectively as shown in Figure 2-4. A plate printed vertically aligns and stacks layers directly bordering above one another. The spacing between surfaces is spaced evenly. Since the machine place beads immediately adjacent to another bead no gap or voids should be present. However, deposited beads are rounded at the edges leaving small voids between corners. Thus full material continuity is not achieved causing a reduction in the generated modulus. Likewise when printing at a 45^0 orientation material

continuity is decreased even further. Having this print angle, not all beads on corresponding surfaces come in contact with one another at the corners.

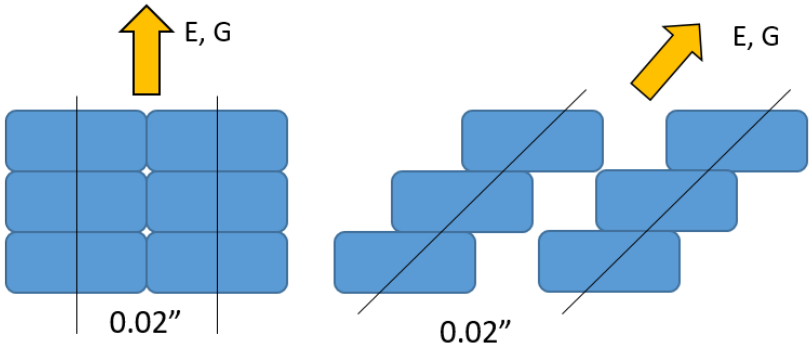

Figure 2-4 Material Discontinuity due to Build Orientation

Since the centerlines are shifted the spacing between beads at this orientation is 1.414 times farther. Due to this increase in distance a larger gap is developed. Under these circumstances, material continuity cannot be kept uniform and an overall significant reduction in modulus is exhibited.

Chapter 3

Methodology

In order to explore the effects of aeroelastic tailoring and scaling stiffness in 3D printed models, a methodology is developed to discuss the varying measured parameters affected. A scaled stiffened plate study model, controlled printing fabrication parameters, testing of configurations, and computational validation through finite element models are discussed in the following sections.

3.1 Scaled Plate Models

From an elastically scaled 3D printed wing structure, stiffened plate models were created to investigate the effects of flexural and twist behavior. The dimensions of the plate are 10 inches by 3.33 inches by 0.5 inches. This represents a $1/10^{th}$ scaling of the wing structure, which has an aspect ratio of 3.0 and an airfoil thickness ratio of 0.15. To investigate the stiffening effects of elastic tailoring, two distinct plate configurations plates are delved into. These two arrangements are 0^0 stiffeners and 45^0 stiffeners. An illustration of both arrangements is shown in Figure 3-1.

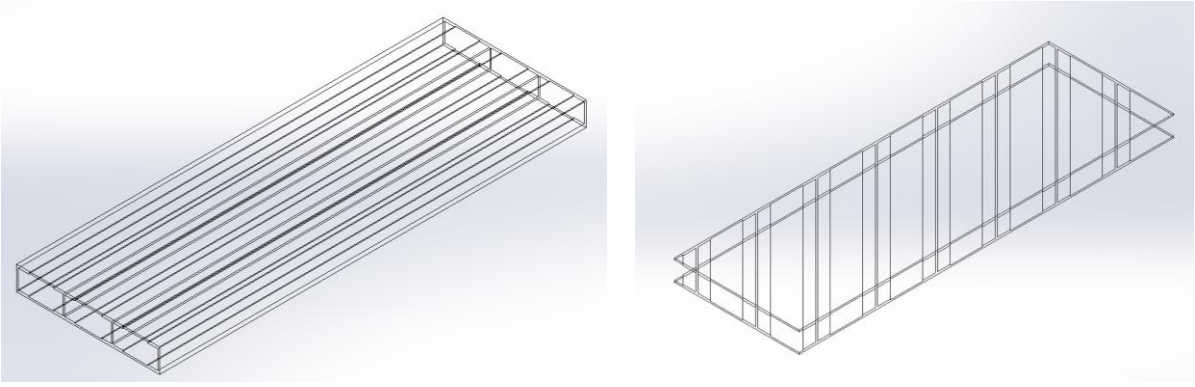

Figure 3-1 Scaled Plate Models in 0^0 and 45^0 Stiffener Arrangements

To keep consistency the stiffeners in both configurations are kept as I beams and are spaced out evenly to match each other. By setting the plates into two simple configurations the behavior they exhibit is suitable for this study.

It is also important to understand how the plate will be printed. The design of the plate is to be printed with individual beads rather than multiple thickened layers. This narrows what effects elastic behavior and focuses the stiffness to be dependent on the bond strength. The printed plate is printed on the Stratasys Fortus 450MC using ABS-M30 which prints at a bead thickness of 0.02 inches. The beads are printed 0.02 inches apart and follow the surface models in Figure 3-1. The skin thickness of the scaled plates is two beads instead of one. This is to maintain model integrity during testing. Two separate thicknesses, two beads and four beads, are studied regarding stiffness effects. The cross section of two bead 0^0 stiffened plate and four bead 0^0 stiffened plate are shown in Figure 3-2 and Figure 3-3.

Figure 3-2 Two Bead 0^0 Stiffened Plate Cross Section

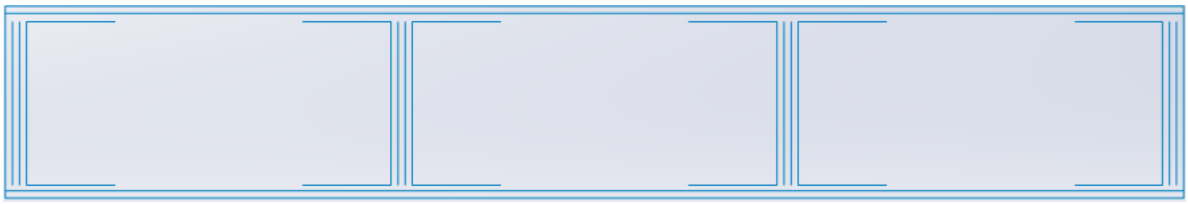

Figure 3-3 Four Bead 0^0 Stiffened Plate Cross Section

The other arrangement requires the stiffeners to be oriented at a 45^0 angle. The centerline distance from the 0^0 stiffened plate is kept for geometric consistency.

3.2 3D Print Orientation

Print orientation in this scenario is not the axes in which a part is built but rather the orientation that the print is being built. Building in different orientations affects how layers bond with each other. Changing the orientation can have many unwanted effects. Specifically, in this case the orientation will affect flexural modulus in the scaled stiffened plates. To determine this effect the plate is printed along the ZX axis in two orientations, vertical and at a 45^0 angle, as shown in Figure 3-4.

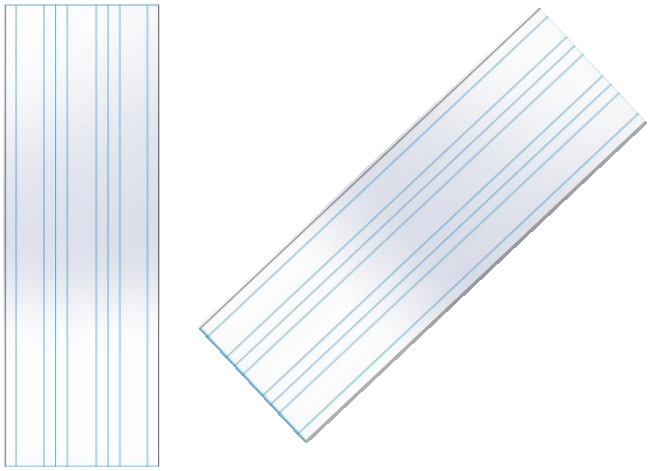

Figure 3-4 Stiffened Scaled Plate Model Orientations

The slicing software utilized is the proprietary software that comes with the Stratasys Fortus 450MC. The slicing software shows the cross-section at different layers and additionally shows in what direction the beads will be placed.

In Figure 3-5, the vertical print can be shown to have adjacent beads with small voids at the top and bottom of the I section. While in Figure 3-6, the 45^0 orientation print will have a gap between beads and between layers as it is built. This continuous buildup of gaps between layers will lower material integrity drastically within the 3D print.

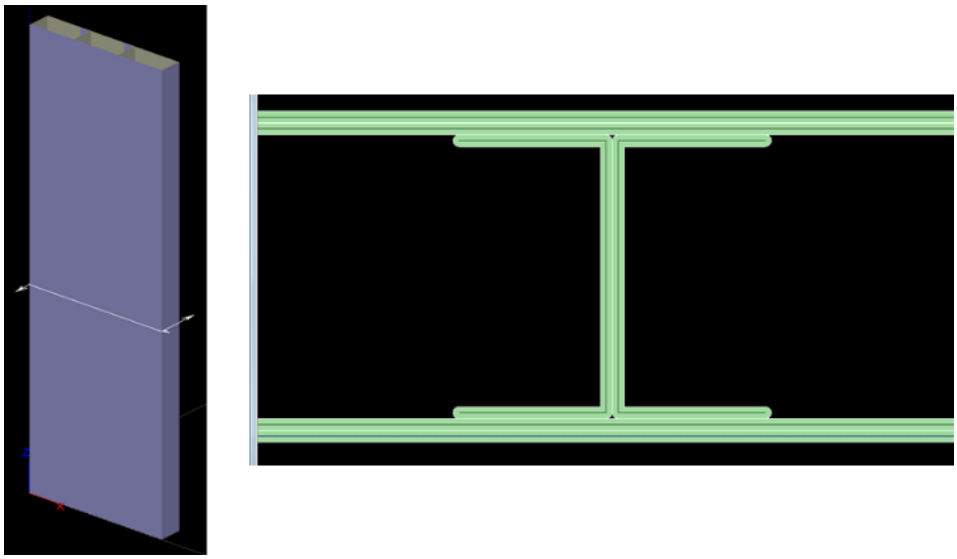

Figure 3-5 Sliced Vertical Stiffened Plate

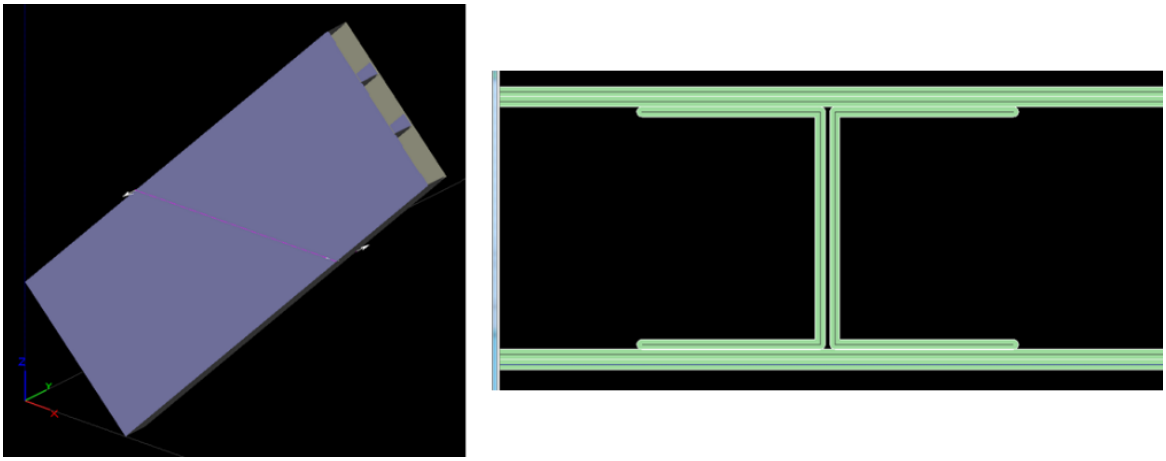

Figure 3-6 Sliced 45^0 Orientation Stiffened Plate

Provided that both print orientations are under the assumption that the extruded material is constant throughout layers and mass is conserved. The reduction in the developed modulus is from the gap in the beads.

3.3 Print Fabrication

As stated earlier the scaled 3D prints were printed on the Stratasys Fortus 450MC. Every possible combination of bead thickness, build arrangement and orientation was printed. A total of eight plates were printed as shown in Figures 9-12. Scaled plate models were printed vertically and at 45^0 orientation at the same time as shown in Figure 3-7. One thing to note is that for the 45^0 configuration for it to be able to be 3D printed two exterior walls were added to sides of the plate. This will have an effect in the results but the data can be manipulated to represent the plate without the extra two walls. Further figures of 3D printed stiffened scaled plate models are in the appendix. Since this is a fused deposition modeling process there was little to no post processing except removing the support material holding the 45^0 oriented stiffened scaled plates.

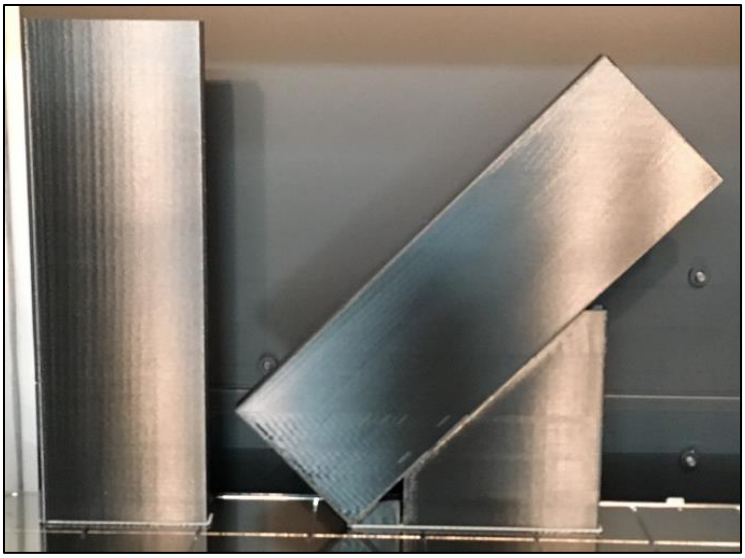

Figure 3-7 3D Printed 0^0 and 45^0 Oriented Stiffened Scaled Plate Models

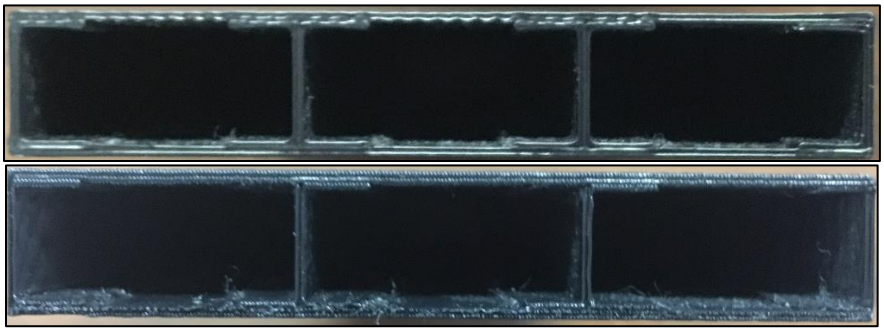

Figure 3-8 2 Bead Stiffeners in 0º Stiffened Plates in 0º (top) and 45º (bottom) Print Orientations

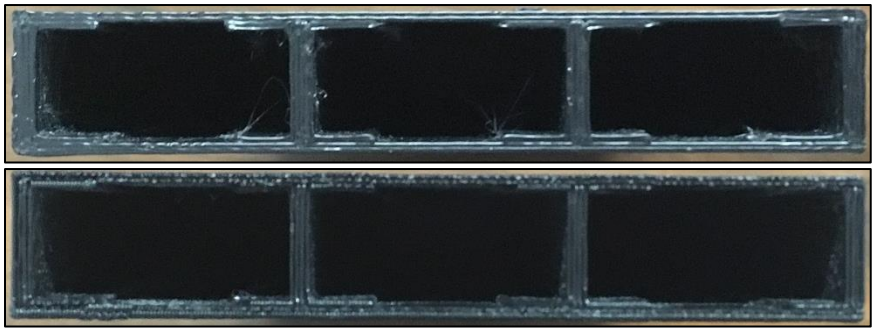

Figure 3-9 4 Bead Stiffeners in 0º Stiffened Plates in 0º (top) and 45º (bottom) Print Orientations

Figure 3-10 2 Bead Stiffeners in 45º Stiffened Plates in 0º (top) and 45º (bottom) Print Orientations

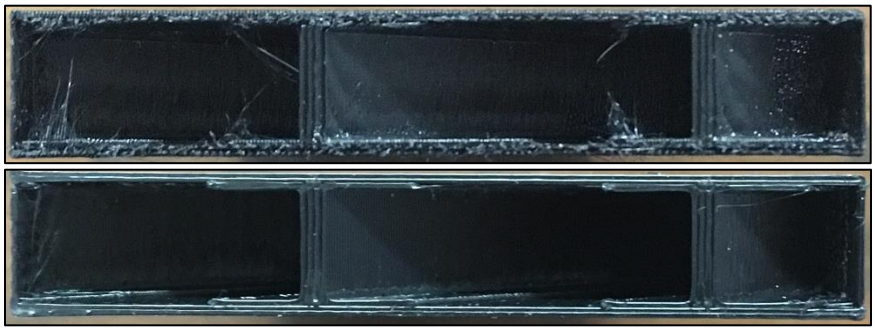

Figure 3-11 4 Bead Stiffeners in 45º Stiffened Plates in 0º (top) and 45º (bottom) Print Orientations

3.4 Plate Testing

In order to investigate the elasticity in the plates the modulus of these scaled 3D printed plates two tests were selected. The scaled 3D printed stiffened plate models were tested under cantilever bend test and three point bend test respectively. Both of these tests rely on the modulus. Making them ideal to determine the mechanical behavior in the plates.

3.4.1 Cantilever Beam Test

A cantilever bend test consists of one end of the beam being anchored while the other end has an applied force as shown in Figure 3-12. For simplicity the stiffeners in the plates are

considered I beams. The formula for calculating the moment of inertia for beam sections is $I = \sum\left(\frac{bh^3}{12} + bhd^2\right)$. The total inertia for the two bead thick plates is 0.025 in^4 and the moment of inertia for the four bead thick plates is 0.026 in^4. Modulus of elasticity is defined by $E_{Elastic} = \frac{PL^3}{3vI}$ where P is the applied force, L is the length of the plate, and v is displacement. However in this scenario, the published modulus for ABS-M30 in the ZX axis is 310,000 psi[20]. Rearranging the equation and solving for displacement the equation becomes $v = \frac{PL^3}{3EI}$. For the length of 8.25 inches and an applied load of 2.205 lbf the predicted displacement for the ideal 2 bead thick plate is approximately 0.06 inches.

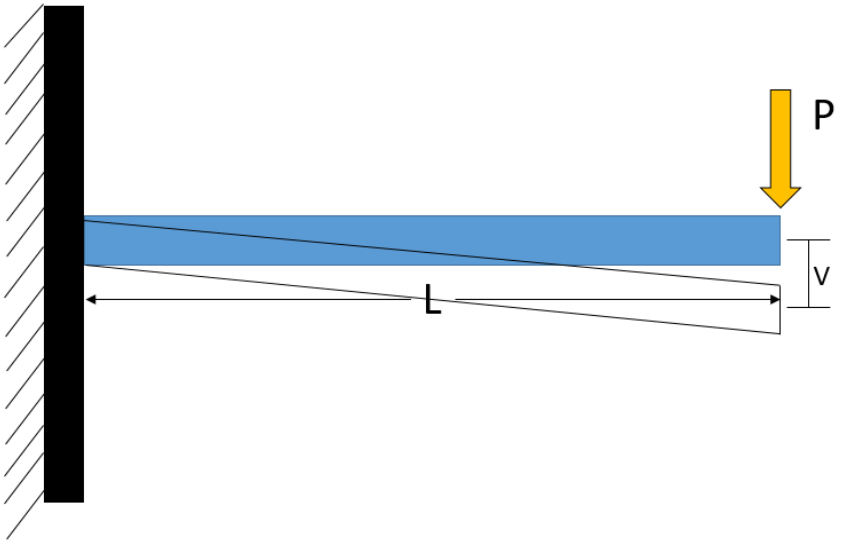

Figure 3-12 Cantilever Bend Free Body Diagram

Now that the concept of cantilever beam test has been defined it is applied to the case study. A setup of the cantilever beam test being performed on a scaled 3D printed stiffened plate

is shown in Figure 3-13. Figures of each individual plate test and fixtures used in the cantilever beam assessment are in the appendix.

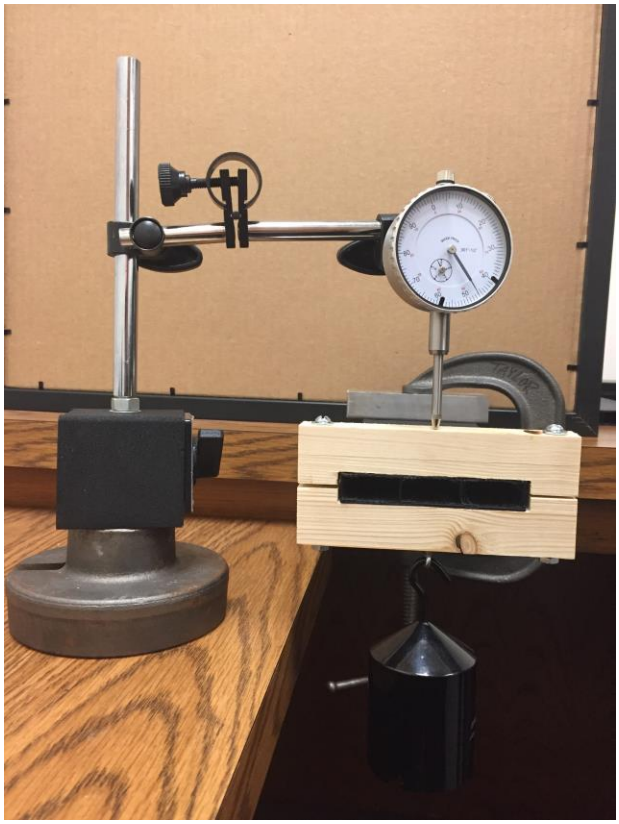

Figure 3-13 Cantilever Bend Test Setup

The scaled 3D printed plates were clamped to the table while the other end had a weight of one kilogram applied. Displacement on the plate was measured using a dial indicator. Measurements were taken at the left corner, center, and right corner at the extremity of the plate. To calculate the displacement a reading was taken when the weight was hinged and then removed. This process was repeated on all applicable 3D printed plates. The modulus from the two bead 0^0 and 45^0 orientation results will act as the primary modulus for all testing purposes.

3.4.2 Three Point Bend Test

The three point bend test is a three point bend test applied on a beam. For this test, the flexural modulus is $E_{Flex} = \frac{PL^3}{48wI}$ where w is the deflection from the applied force as shown in Figure 3-14. Rearranging the equation and solving for deflection the equation becomes $w = \frac{PL^3}{48EI}$. The three point bend test performed was setup to have a length, L, of 7.0 inches and an applied force of 18.0 lbf. The predicted deflection of an ideal 2 bead thick plate is 0.018 inches.

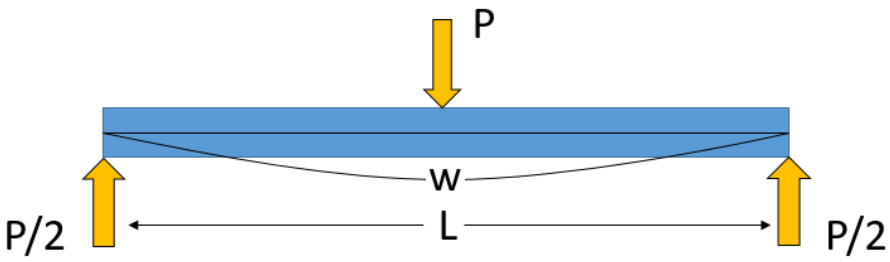

Figure 3-14 Three point Bend Free Body Diagram

The setup of the performed three point bend test can be seen in Figure 3-15. The Shimadzu Autograph model AGS-X universal was the testing machine. In the three point bend tests only 0^0 arranged stiffeners were calculated. The 45^0 arranged stiffener plates have an added component of twist that offset the results if performed with this test.

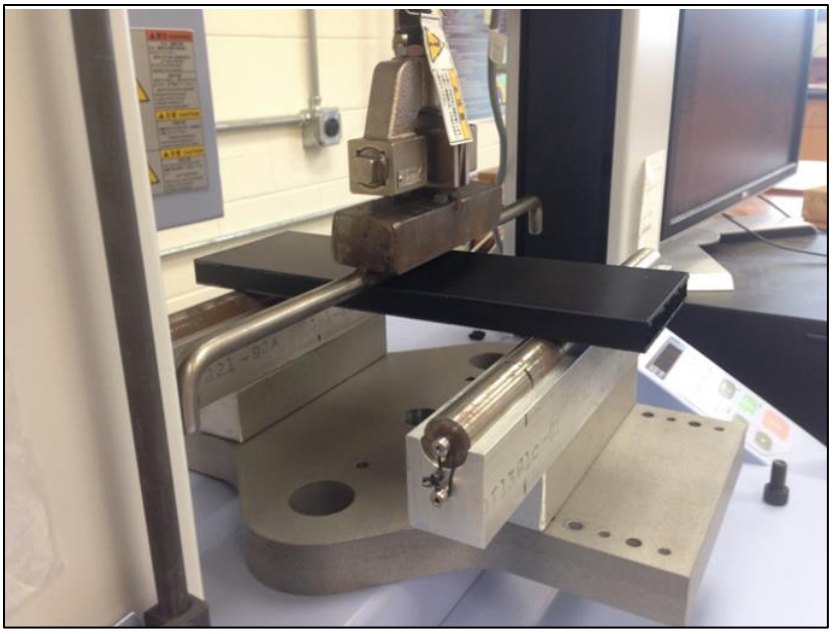

Figure 3-15 Three Point Bend Test Setup

The 3D Printed stiffened plates were placed on the rollers of the three point bend fixture. As an applied force is making contact with the plate the hydraulic press sends data back to the computer with how much the stiffened plate has deflected.

3.5 Finite Element Models

The same scaled 3D printed stiffened plate models were modeled in Altair HyperMesh. When dealing with finite element software a few assumptions must be stated. For instance, the Altair HyperMesh software assumes that perfect bonding between layers occurs but that is not the case as discussed in section 3.2. Furthermore, since the stiffened plate models are represented as 100% material continuity the weaker modulus from building at an angled orientation is not reproduced during the analysis.

To try and mimic the thin surfaces and beads of the 3D printed stiffened plate models the HyperMesh models were created as shell models. Since these models are simplified the models

contain fewer elements which in turn decreases the computing time. These models are analyzed as having fully developed modulus. A cross section of the simplified model is shown in Figure 3-16.

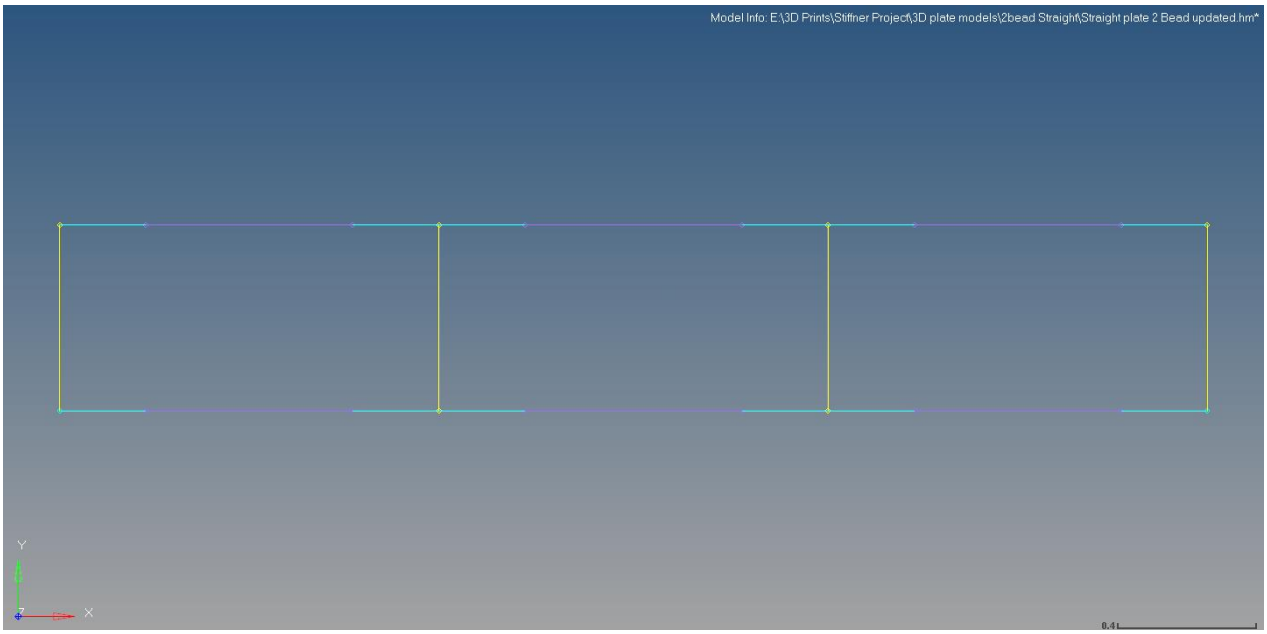

Figure 3-16 Scaled Stiffened Plate Model Cross-Section

Once the model is created it is then meshed to a suitable fine mesh. The 0^0 scaled stiffened plate model has a quad element style mesh while the 45^0 model has a mix of quad elements and triangular.

The model can be separated into categories for each surface. The purple colored surfaces represent the exterior surface thickness. The blue colored surface represent the flanges on the stiffeners. Lastly, the yellow colored surfaces represent the stiffeners. These colored surface are illustrated in the 0^0 scaled stiffened plate model shown in Figure 3-17 and the 45^0 scaled stiffened plate model shown in Figure 3-18.

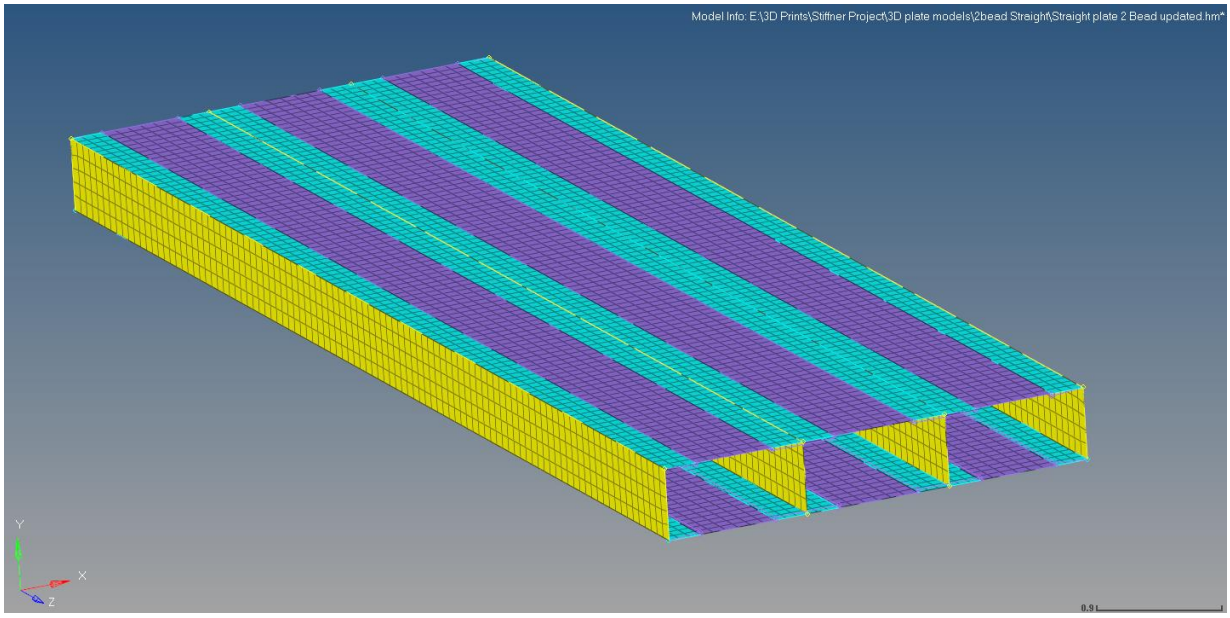

Figure 3-17 0^0 Scaled Stiffened Plate Model Mesh

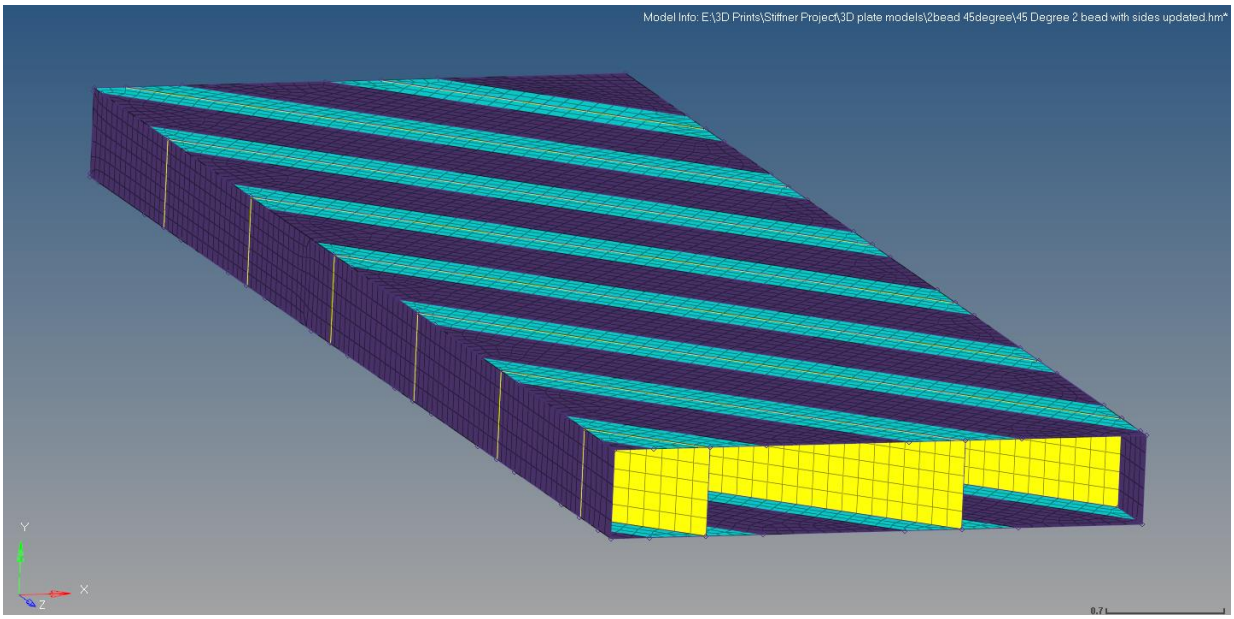

Figure 3-18 45^0 Scaled Stiffened Plate Model Mesh

As shown in Figure 3-19 and Figure 3-20, these categories of surfaces are given a thickness corresponding to the original scaled 3D printed plate. The thicknesses correspond to

the dimensions stated in section 3.1. Flange and surface regions of the model used z-offsets to correctly position the thickness.

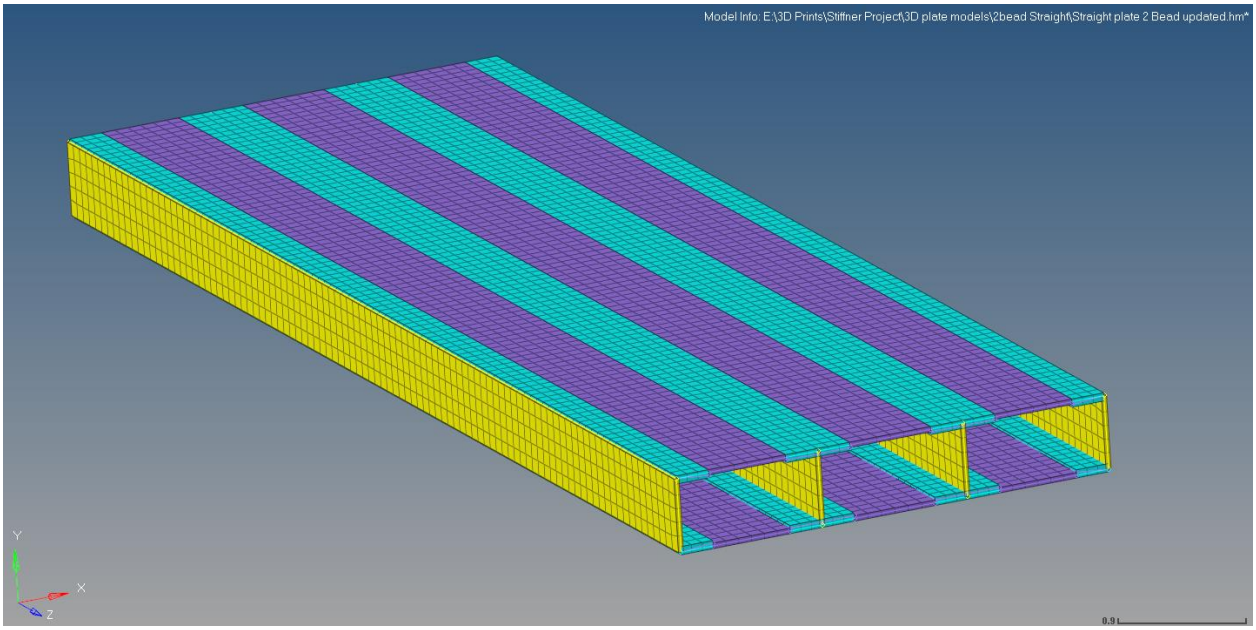

Figure 3-19 0^0 2 Bead Thick Scaled Stiffened Plate Model Mesh

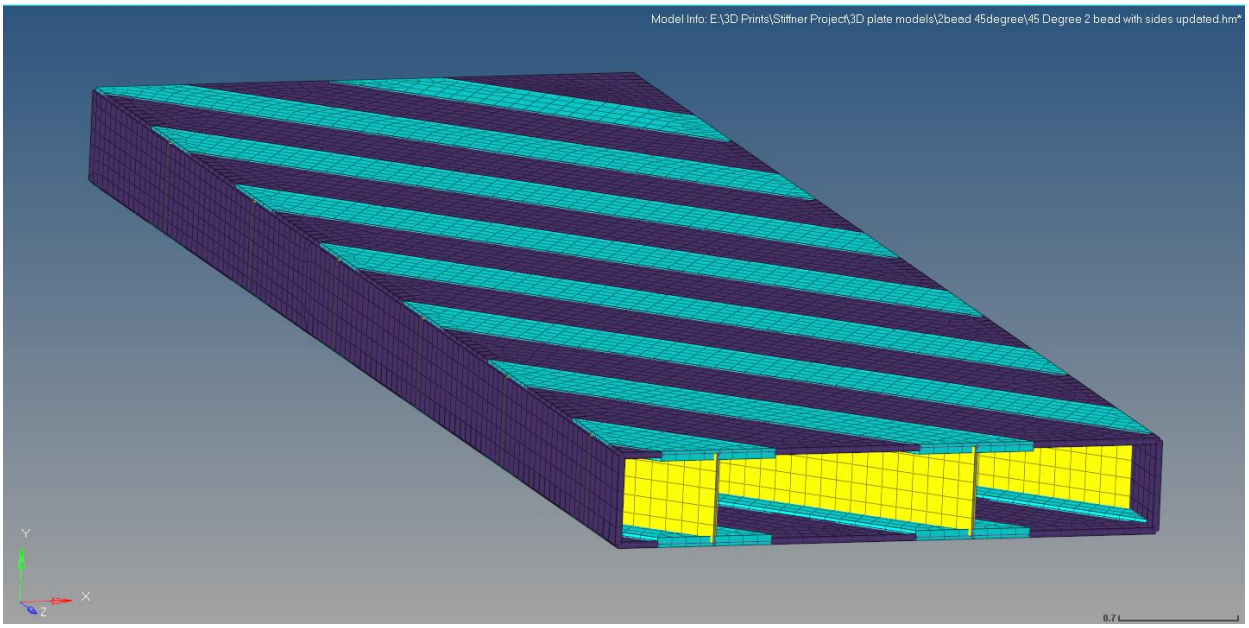

Figure 3-20 45^0 2 Bead Thick Scaled Stiffened Plate Model Mesh

The last thing that needs to be defined before creating constraints and loads on the model are the material properties. The material properties for the models are from the established Stratasys ABS-M30 properties shown in Table 3-1. As mentioned earlier the finite element analysis software assumes fully bonded layers. Therefore the material properties established will be significantly higher than the experimental results. In order to get an accurate representation the modulus obtained from the cantilever tests at 0^0 and 45^0 orientation will be used for both model tests.

Table 3-1: ABS-M30 Mechanical Properties in ZX Axis[20]

Mechanical Properties	Value	Units
Tensile Strength, Yield	3,750	psi
Tensile Strength, Ultimate	4,050	psi
Tensile Modulus	310,000	psi
Poisson's Ratio	0.35	
Elongation at Break	2%	
Elongation at Yield	1%	

Table 3-2: Modulus for 0^0 and 45^0 orientations

Build orientation	Modulus, lbf/in^2
0º	188,000
45º	167,450

Note that there is an 11% in reduction in modulus when printing at 45^0 orientation. Next conditions and loads were applied to the finite element models. The loads and conditions are the same as stated in section 3.4.

In the cantilever bend test the top and bottom surface on one end is completely fixed. The constraints were defined by fixing all degrees of freedom (DOF 123456). To simulate a single

force applied at the end of the plate and along the edge a single node made from an RBE3 is used. Displacement results were extracted from the tip midpoint on the top surface.

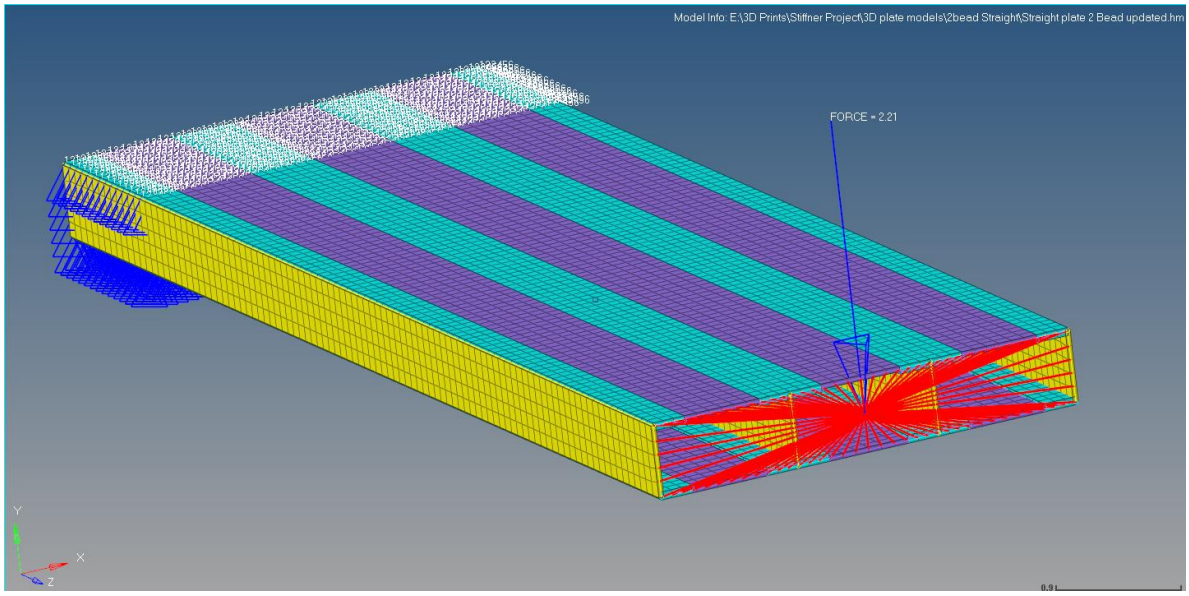

Figure 3-21 0^0 2 Bead Thick Scaled Stiffened Plate Model Mesh Cantilever Test

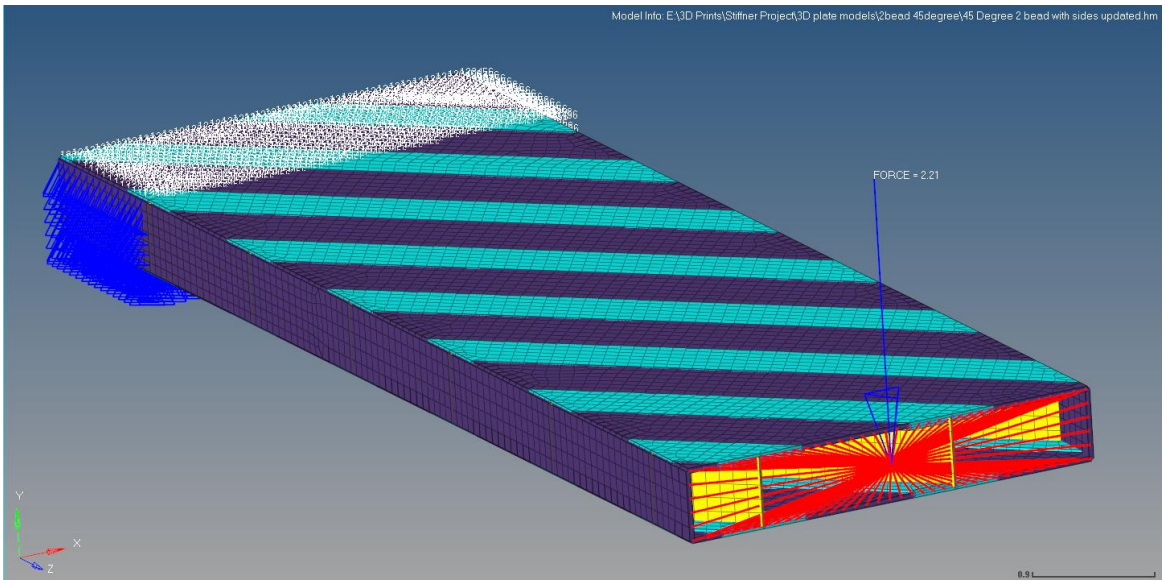

Figure 3-22 45^0 2 Bead Thick Scaled Stiffened Plate Model Mesh Cantilever Test

On the other hand the three point bend test has two constraints on the bottom surface near the ends of the plate. The constraints spaced at seven inches apart were defined by fixing

translation (DOF 123). The upper surface has four loads acting at each stiffener to simulate the total force applied in a three point bend test.

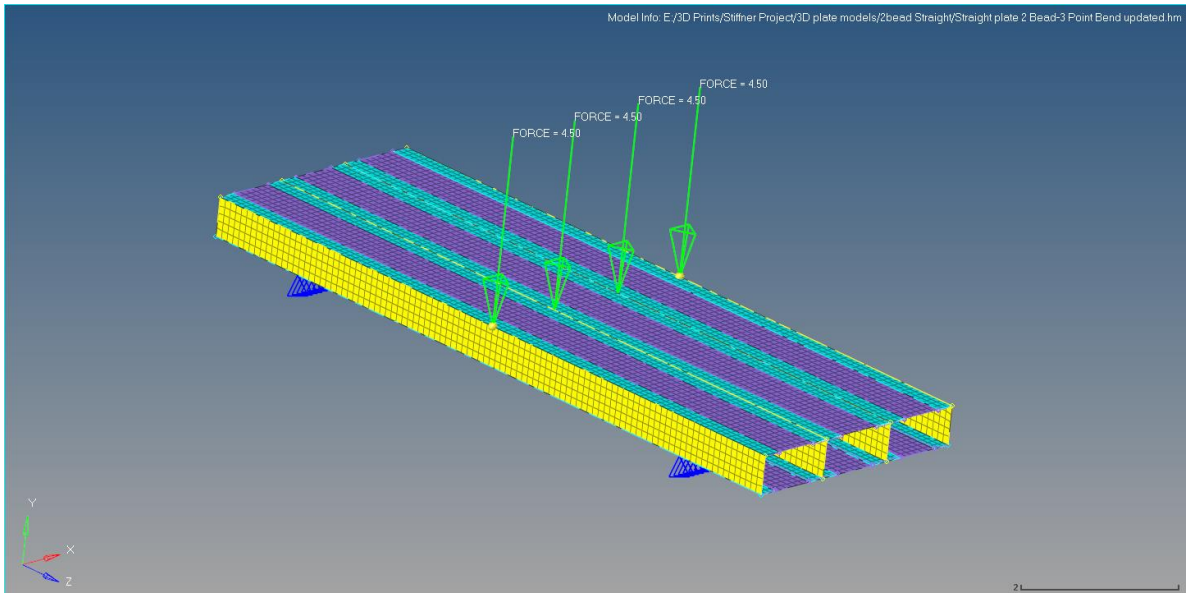

Figure 3-23 0^0 2 Bead Thick Scaled Stiffened Plate Model Mesh 3 Point Bend Test

Chapter 4

Results and Discussion

The experimental and computational tests conducted were done in order to evaluate how stiffness is affected by bead thickness, geometric configurations, and different build orientations. Every possible combination of parameter is investigated. In this section the results are broken into three main sections. The experimental results discuss the physical testing done. The computational results discuss how finite element analysis can be applied to calculate the expected behavior. Then both of the results are compared to see if similar results between them were achieved.

4.1 Experimental Results

The experimental tests conducted are the three point bend and cantilever beam tests.

4.1.1 Three point bend results

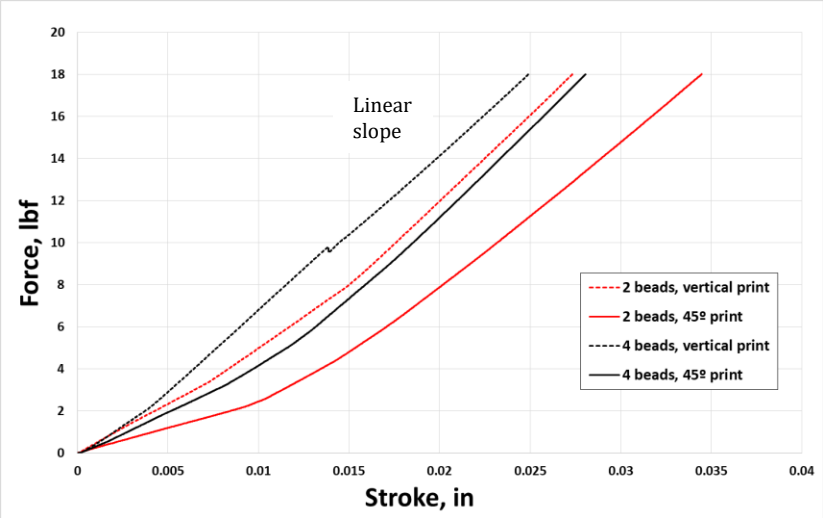

Figure 4-1 Three Point Bend Results

For 0^0 stiffened scaled plate models the three point bend testing yielded force vs. stroke. Looking at the data in the Figure 4-1 the displacement is nonlinear and then transitions into

linear once above 10lbf. Note that the small down shift in the four bead vertical plate is from the cracking in the layers. This non linearity plays a significant factor in the increase of displacement as the load is increased. The connection between nonlinearity and the stiffness of the plate along with material continuity are all printing induced effects. Displacements of the 3 point bend test are shown in Table 4-1.

Table 4-1: Experimental Three Point Bend Modulus Results

Configuration	Displacement, in	Calculated Modulus, E psi	Modulus reduction, %
2 bead, 0º print	0.027	191506.5	20.7
2 bead, 45º print	0.034	151847.2	
4 bead, 0º print	0.025	196814.8	11.2
4 bead, 45º print	0.028	174706.0	

Notice that in the two bead and four bead thick stiffened scaled plates there is a reduction in stiffness due to build orientation. This correlates back to section 3.2 in which the gap between the beads limits the bond strength between layers. From Table 4-1 it is clear that building at a 45^0 orientation causes a significant reduction in flexural stiffness.

4.1.2 Cantilever beam results

The cantilever beam testing yielded displacements for the 0^0 and 45^0 stiffened scaled plate models. The cantilever tests results for 0^0 stiffened plates can be seen in Table 4-2. The displacements were measured with and without the applied load from the dial indicator at three different points. From these measurements the net displacement, average displacement, and angle of twist were calculated. The measuring was done with tools mentioned in section 3.4.1. The dial was moved from right to left and the weight was added and removed to determine the displacement. With the displacement results the calculations for flexural modulus can be made.

Table 4-2: Cantilever Test Results for 0^0 Stiffened Plates

Configuration	Dial Reading		Net Displacement, in	Angle, deg	Average Displacement, in	Calculated Modulus, E psi	Modulus Reduction, %
	No Load	2.20 lbf					
2 bead, 0º Orientation							11.2
Right	0.111	0.021	0.09	0.019	0.09	187,420.90	
Middle	0.128	0.04	0.088				
Left	0.141	0.05	0.091				
2 bead, 45º Orientation							
Right	0.14	0.04	0.100	0.057	0.101	166,390.20	
Middle	0.148	0.048	0.100				
Left	0.151	0.048	0.103				
4 bead, 0º Orientation							11.0
Right	0.087	0.006	0.081	0.095	0.083	1888,59.5	
Middle	0.09	0.007	0.083				
Left	0.129	0.043	0.086				
4 bead, 45º Orientation							
Right	0.118	0.025	0.093	0.076	0.094	168,024.50	
Middle	0.134	0.043	0.091				
Left	0.146	0.049	0.097				

Table 4-3: Cantilever Test Results for 45^0 Stiffened Plates

Configuration	Dial Reading		Net Displacement, in	Angle, deg	Average Displacement, in
	No Load	2.20 lbf			
2 bead, 0º Orientation					
Right	0.224	0.054	0.17	-0.306	0.161
Middle	0.236	0.076	0.16		
Left	0.251	0.097	0.154		
2 bead, 45º Orientation					
Right	0.213	0.061	0.152	0.019	0.155
Middle	0.230	0.071	0.159		
Left	0.237	0.084	0.153		
4 bead, 0º Orientation					
Right	0.240	0.105	0.135	0.019	0.136
Middle	0.249	0.111	0.138		
Left	0.261	0.125	0.136		
4 bead, 45º Orientation					
Right	0.213	0.084	0.129	-0.012	0.127
Middle	0.230	0.101	0.129		
Left	0.243	0.100	0.123		

Table 4-3 displays the cantilever test results for 45^0. The exact same testing procedure on the 0^0 stiffened plates were done to this set. One thing that was apparent in testing the 45^0 configuration prints is that there was no twisting. This zero twisting should not be happening because of how the stiffeners are configured. These 45^0 stiffened plates require a stiffness matrix in order to calculate accurate moduli. The main cause of this issue is rooted at the fact that the test is dependent on the moments of inertia. Having this added angle on the stiffeners completely changes the test and does not appropriately represent the actual behavior.

4.2 Computational Results

Displacement results were generated for the 0^0 and 45^0 finite element model plates. For all 0^0 oriented plates, a modulus of 188,000 psi was used. This value stems from the early cantilever test. This modulus represents the actual 3D printed stiffened plates. For all 45^0 oriented plates, the modulus was reduced by 11% to 167,450 psi to account for the larger gap between beads.

4.2.1 Finite Element Three point bend results

The resulting displacements in the two bead and four bead 0^0 stiffened scaled 3D plates from the three point bend tests are shown in Figure 4-2 and Figure 4-3. The max displacement for the two bead 0^0 stiffened scaled 3D model is 0.0319 inches located at the center of the plate along the edges. It is interesting to see that the outer side walls have a higher displacement than the inner stiffeners. This region has higher displacements due to how the forces were applied on the model. To obtain a uniform distribution a work equivalent force distribution would need to be applied. The max displacement in the four bead 0^0 stiffened scaled model is 0.0267 inches.

The lower displacement is from having thicker stiffeners. Due to the increased thickness the added beads increase the bond strength and has a significant flexural stiffness increase.

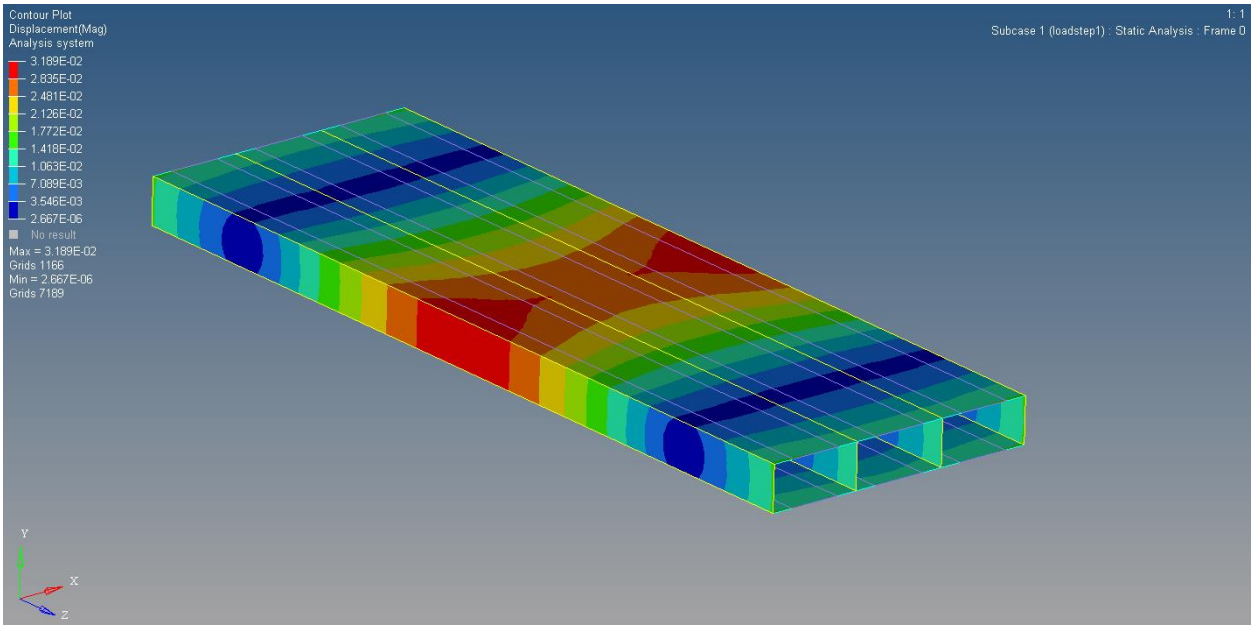

Figure 4-2 2 Bead 0^0 Configuration & 0^0 Orientation Three Point Bend Contour Plot

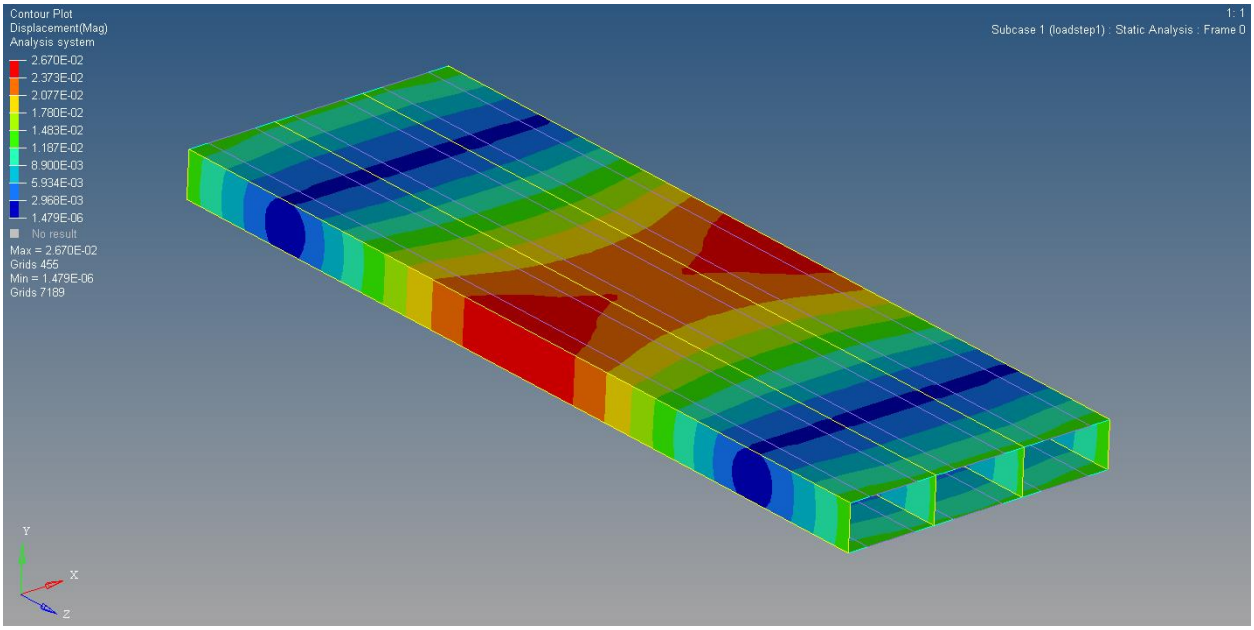

Figure 4-3 4 Bead 0^0 Configuration & 0^0 Orientation Three Point Bend Contour Plot

Table 4-4: Three Point Bend Finite Element Results for 0^0 Stiffened Plate Models

Configuration	Test Displacement, in	FE Displacement, in	Percent Difference, %
2 bead, 0º Orientation	0.027	0.027	0.82
2 bead, 45º Orientation	0.034	0.030	11.78
4 bead, 0º Orientation	0.025	0.023	7.63
4 bead, 45º Orientation	0.028	0.026	7.31

In table 4-4 a comparison is done between the measured test and the finite element model for the three point bend tests for 0^0 stiffened plates. With the modulus of 188,000 psi for the 0^0 orientations the difference were reasonable but not ideal for an acceptable methodology. Notice that the displacements from the finite element models follow the pattern where the 45^0 orientation leads to more deflection. This causes a significantly higher difference between both results.

4.2.2 Finite Element Cantilever beam results

The cantilever beam results for 0^0 and 45^0 stiffened scaled 3D plates with two and four bead thick stiffeners are discussed in this section. In Figure 4-4 the max displacement is happening on the farthest most edge. The displacement there is 0.0913 inches. This amount of displacement is larger than the ideal calculated in section 3.4.2. The higher displacement is caused by the fact that the plate consists of thin walls and has stiffeners of bead thickness of two.

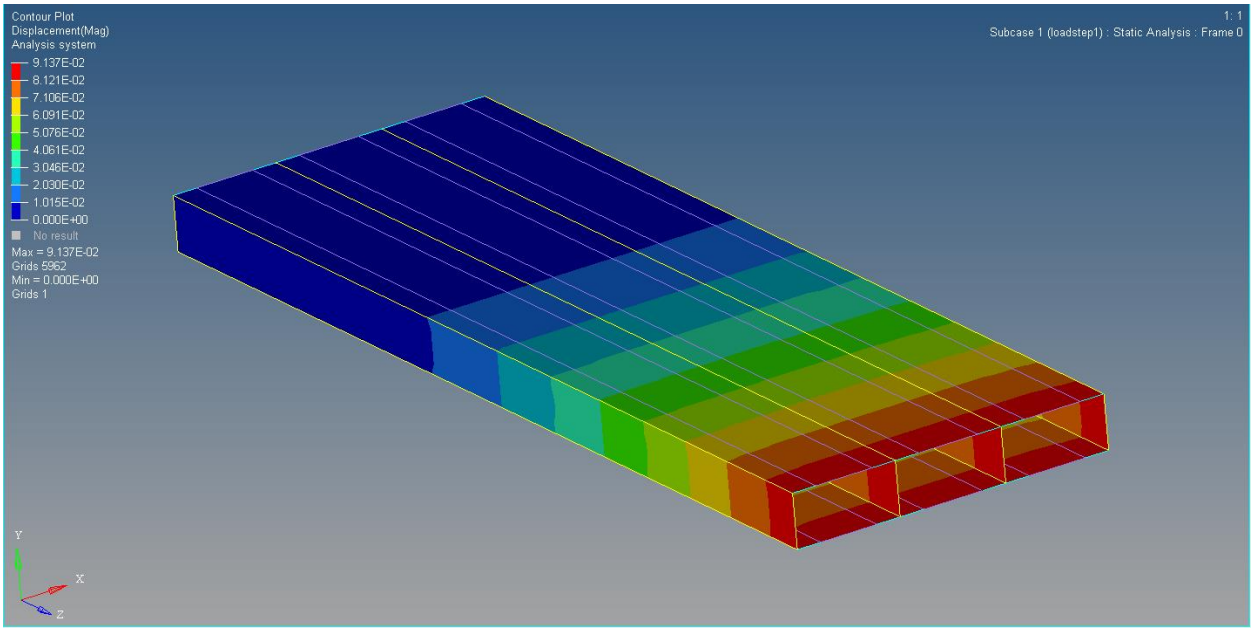

Figure 4-4 2 Bead 0^0 Configuration & 0^0 Orientation Cantilever Contour Plot

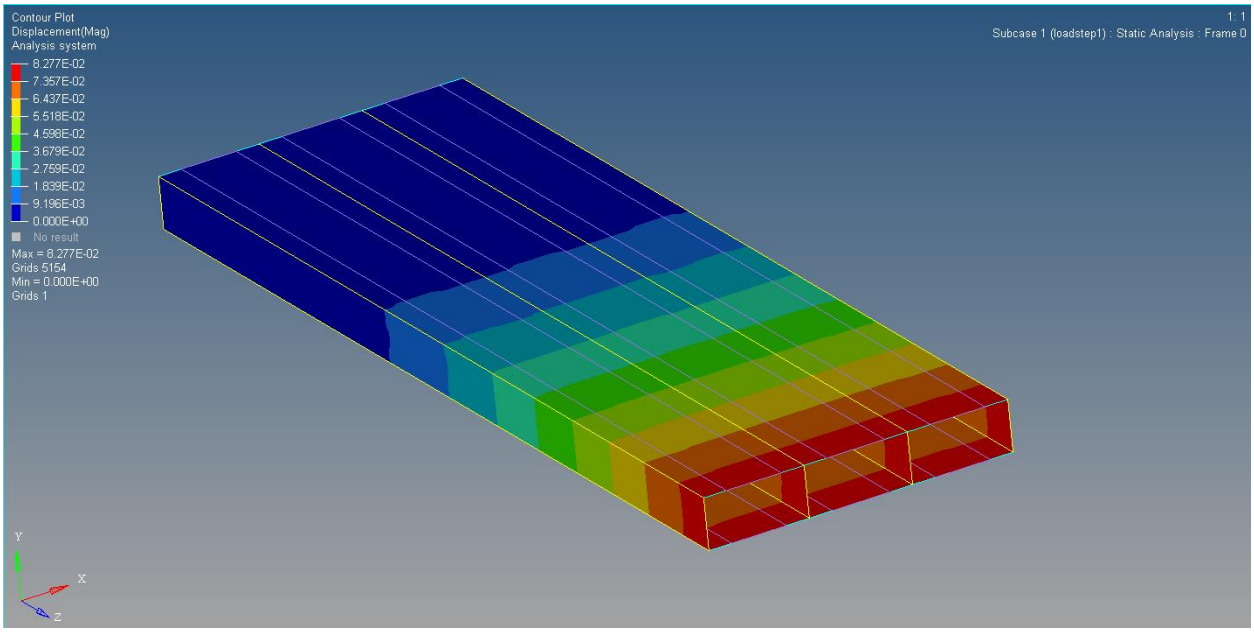

Figure 4-5 4 Bead 0^0 Configuration & 0^0 Orientation Cantilever Contour Plot

Coincidently the 0^0 four bead thick scaled stiffened plate model also has a notable increase in displacement when compared to the ideal. The max displacement occurring in the

four bead thick model is 0.083 inches. From previous tests there is a relation that continues to be seen and that is when bead thickness is increased there is also an increase in flexural stiffness. Table 4-5 continues to follow the established trend that the orientation is the cause for having higher displacement.

Table 4-5: Cantilever Beam Finite Element results for 0^0 Stiffened Plate Models

Configuration	Test Displacement, (in)	FE Displacement, (in)	Percent Difference, %
2 bead, 0º Orientation	0.090	0.089	1.11
2 bead, 45º Orientation	0.101	0.100	0.99
4 bead, 0º Orientation	0.083	0.081	2.41
4 bead, 45º Orientation	0.094	0.091	3.19

In table 4-5 a comparison is done between the measured test and the finite element model for the cantilever beam tests for 0^0 stiffened plates.

Even more, the 45^0 configuration scaled stiffened plate models have the same behavior as the 0^0 configuration scaled models. However, unlike the 0^0 configuration scaled stiffened plates max displacement is not uniform on the free end. The angled stiffener produces coupling bending and twisting deformation and that is what is observed. In Figure 4-6 and 4-7, the displacement regions are angled and are mostly concentrated where the stiffeners reach the end of the top and bottom surfaces. If a third stiffener on the right side had reached the limit of the plate a more uniform displacement would occur.

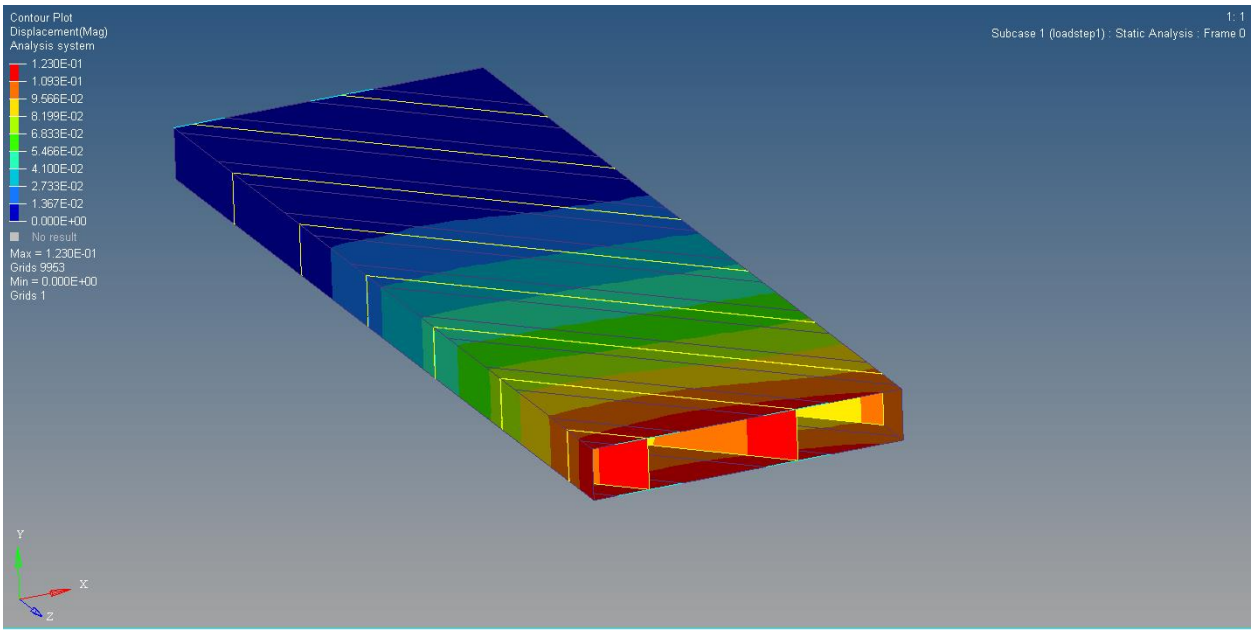

Figure 4-6 2 Bead 45^0 Configuration & 0^0 Orientation Cantilever Contour Plot

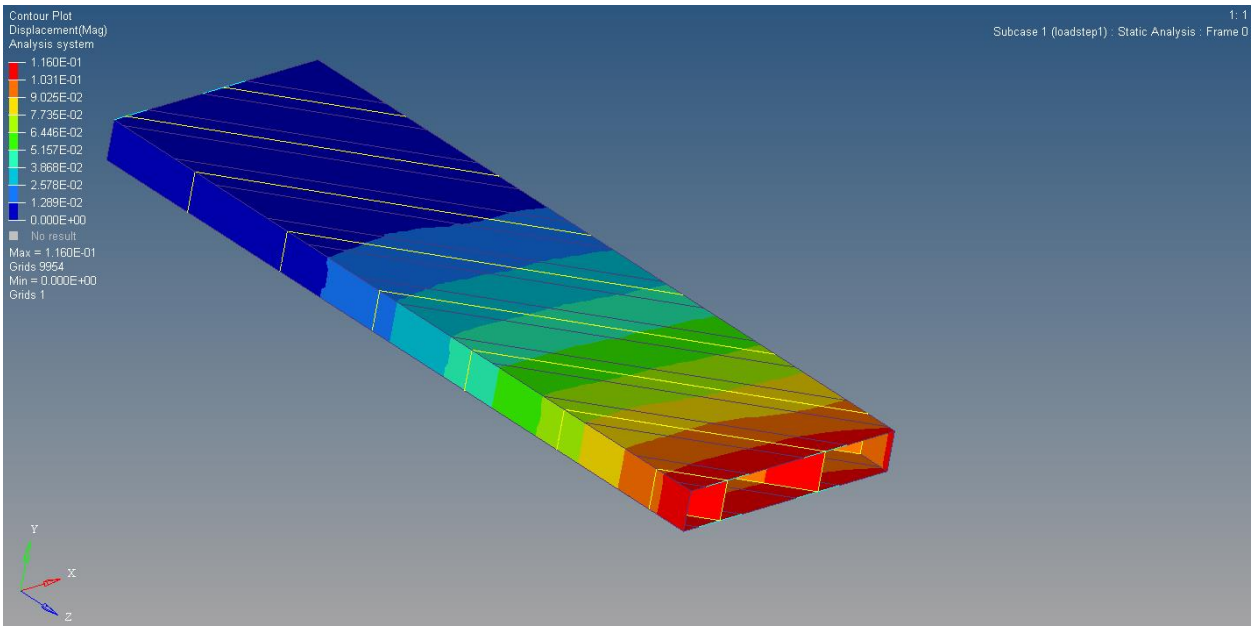

Figure 4-7 4 Bead 45^0 Configuration & 0^0 Orientation Cantilever Contour Plot

In Figure 4-6, the max displacement is 0.12 inches. This is higher than the ideal displacement for this test. Going from two bead to four bead stiffeners has a positive impact on

the stiffness. Specifically, for the 45^0 configuration plate the percent difference is not as great as seen in the 0^0 configuration plate models.

Table 4-6: Cantilever Beam Finite Element results for 45^0 Stiffened Plate Models

Configuration	Test Displacement, (in)	FE Displacement, (in)	Percent Difference, %
2 bead, 0º print	0.161	0.110	31.68
2 bead, 45º print	0.155	0.123	20.65
4 bead, 0º print	0.136	0.105	22.79
4 bead, 45º print	0.127	0.118	7.09

In table 4-6 a comparison is done between the measured test and the finite element model for the cantilever beam tests for 45^0 stiffened plates. Utilizing the calculated modulus, all of the values were significantly different. Making this a very poor comparison between these plates. Additionally, the twisting component that is supposed to happen because of inherent effects of the angled configuration is not occurring and can be seen in Figure 4-6 and Figure 4-7.

When comparing the two and four bead thick 0^0 and 45^0 configurations the displacement difference between them is small. The 45^0 orientation tended to have higher displacements which results in a lower flexural stiffness. This closely follows the trend that has been happening in the calculated results.

Looking at the experimental and computational values for the finite element models and experimental test they exhibited similar behavior. For this methodology to be acceptable the idea is to have minimal difference between values. The smaller the difference the more accurate the results. The idea is to run iterations of these tests until achieving a percent difference lower than 1%. Comparing both of the results it is clear that the 45^0 configurations in the experimental approach had significant differences when compared to the computational approach. It is clear that the 45^0 configuration stiffened scaled plates are not represented properly by the experimental

calculations. The angled stiffeners were not properly calculated with simple moment of inertia calculations. A more theoretical approach would be needed.

Chapter 5

Conclusion

The objective of this research was to develop a process that enables elastically scaled 3D printed models built through fused deposition modeling to be calibrated and tuned. The work done is a first attempt at this methodology. From the experimental calculations it is clear that the methods utilized for calculating flexural modulus rely on the printed models assumption in having full material integrity. However, it is seen in the actual results that the 3D scaled stiffened plates have voids and gaps between beads and layers. When validating the experimental results to the finite element analysis the increased displacement occurring when printing at an angle is further exhibited. The increased displacement in turn influences the flexural modulus and affects the effective stiffness.

From the results it is clear that printing along the ZX axis at a 0^0 orientation instead of a 45^0 orientation resulted in an accurate representation of having a fully developed modulus. Subsequently, printing at this orientation revealed how significant bond adhesion between layers plays a considerable component in elastic tailoring. However, print orientation was not the most influential factor in maintaining stiffness. Comparing between the two build configurations the calculations gravitated towards higher displacements when going from vertical stiffeners to 45^0 stiffeners. This noticeable increase in displacement supports how configuration drastically alters flexural modulus. The most apparent influence in stiffness from the results was the bead thickness. By just adding another bead stiffness was passively increased substantially. Therefore, bead thickness and build configuration were significantly the driving parameters in this case.

The initial methodology was proven to be lacking and was limited in the fact that a fundamental modulus backed by testing of mechanical properties needed to be the driving factor.

The variations in results show the poor correlation between tests and finite element models. The major problems stem from the initial approach taken. A more fundamental approach starting from dog bone specimens to determine the stiffness and the effect it has on material continuity would be the starting point. With further work a more reliable and solid methodology can be adapted. In spite of the needed modulus the methodology provided the means to distinguish the key parameters required to tune and tailor the elastically scaled 3D printed plates.

Chapter 6

Future work

There are plenty of studies that would have been beneficial to the paper but, were not included do to time constraints. Here are a few examples that would help with reinforcing this study. Printing tensile specimens at desired orientations and then testing to measure tensile strength and modulus. This would be really beneficial when trying to do measure the tensile modulus for various oriented prints. Additionally it would reinforce the behavior happening in the finite element analysis. Another possibility is 3D printing more models at various print orientations and print configurations in order to investigate and fine tune the process. Furthermore, having varying amounts of stiffeners in the 3D printed plates should be investigated as well. The change in stiffeners could definitely impact the overall stiffness. In the calculations for moment of inertia the stiffeners and flanges had an influence on the beam tests. Possibly having a more formulated theoretical approach on obtaining the moments of inertia for angled stiffeners would increase precision and accuracy in those tests. Lastly, changing the geometry of the stiffeners and determining the effect it has on the stiffness could be investigated.

Appendix

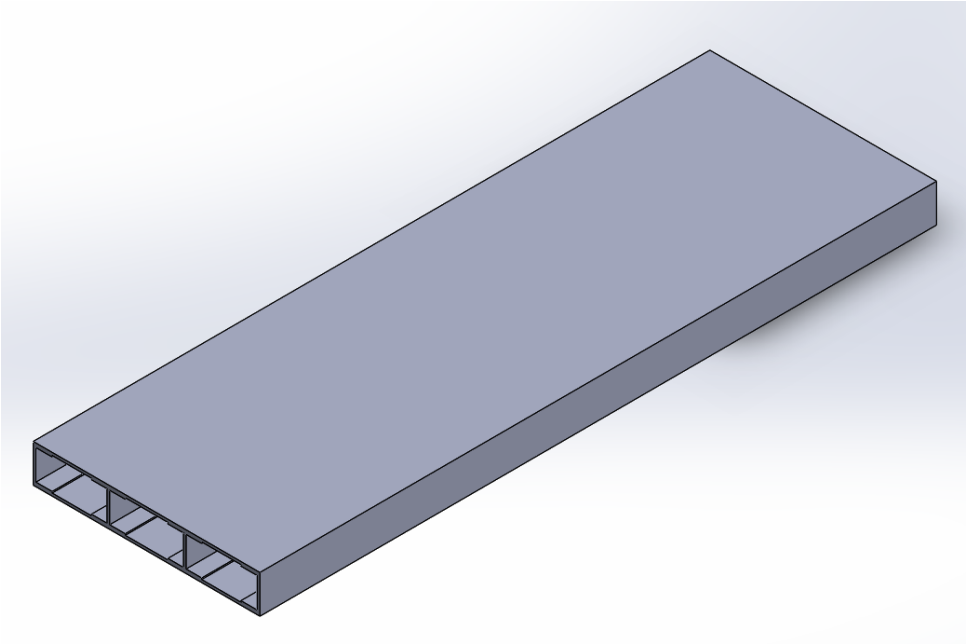

Figure A-1 2 Bead 0^0 Stiffened Plate Model

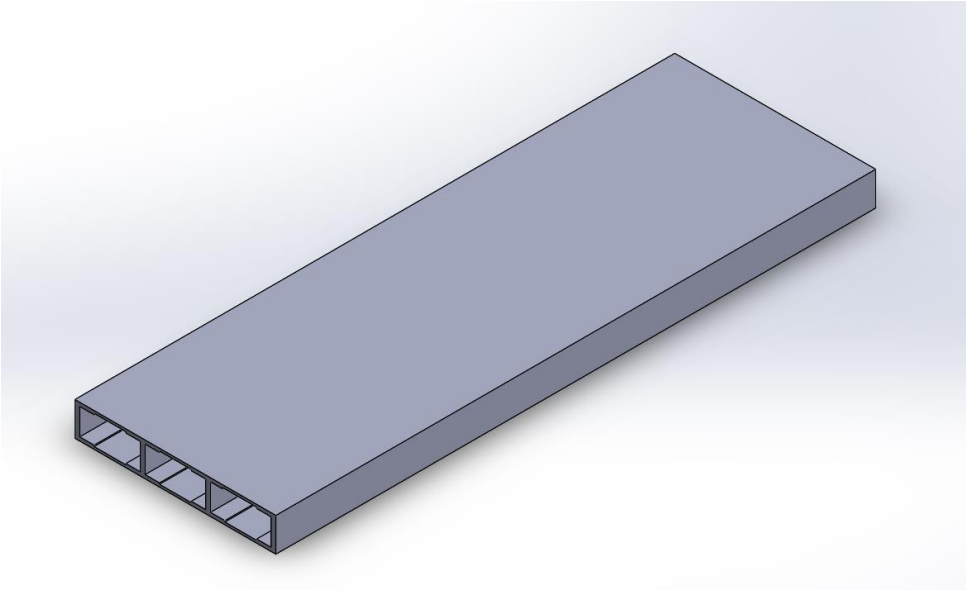

Figure A-2 4 Bead 0^0 Stiffened Plate Model

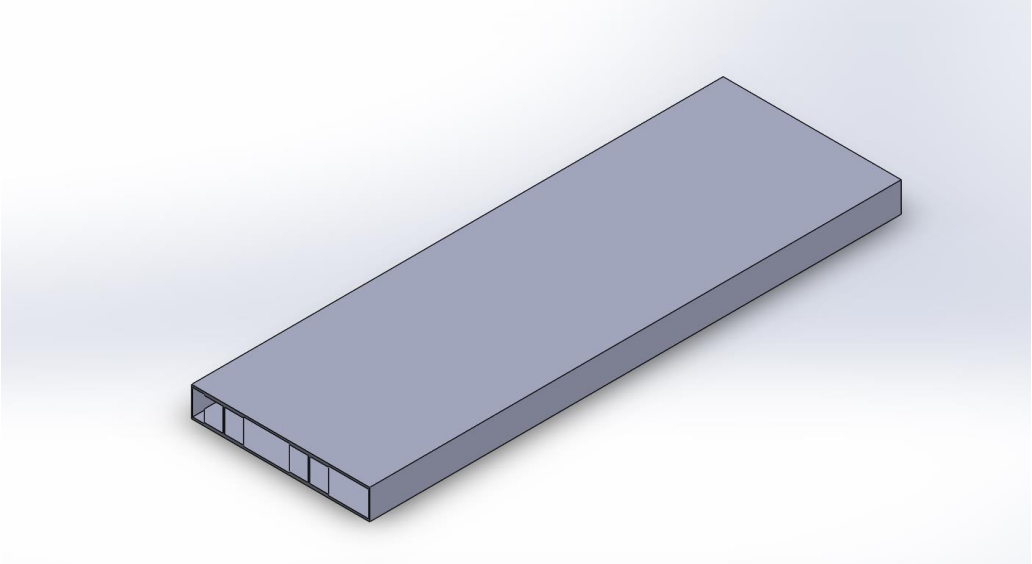

Figure A-3 2 Bead 45^0 Stiffened Plate Model

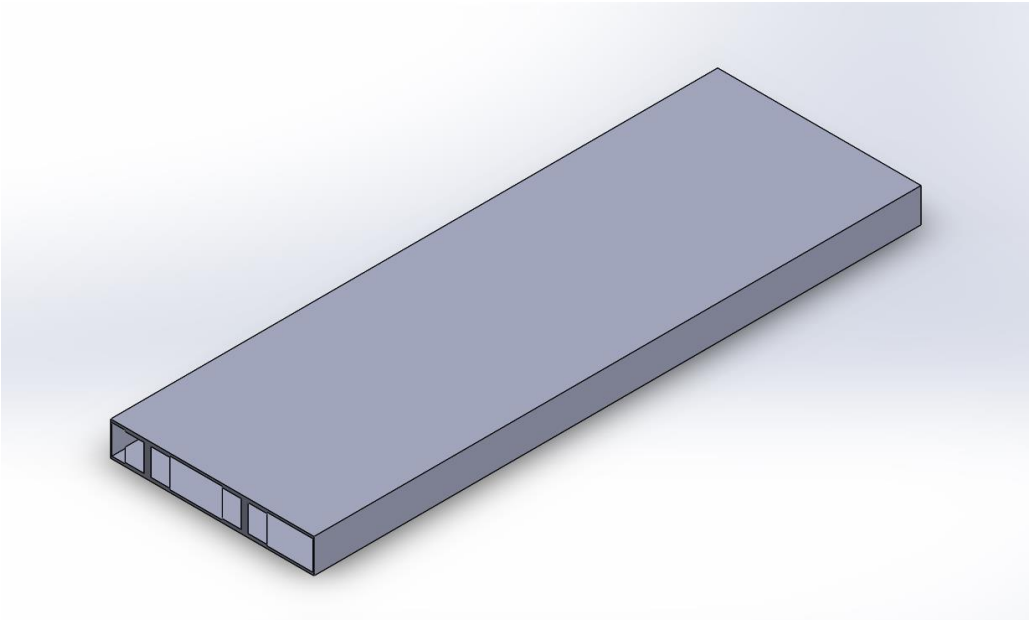

Figure A-4 4 Bead 45^0 Stiffened Plate Model

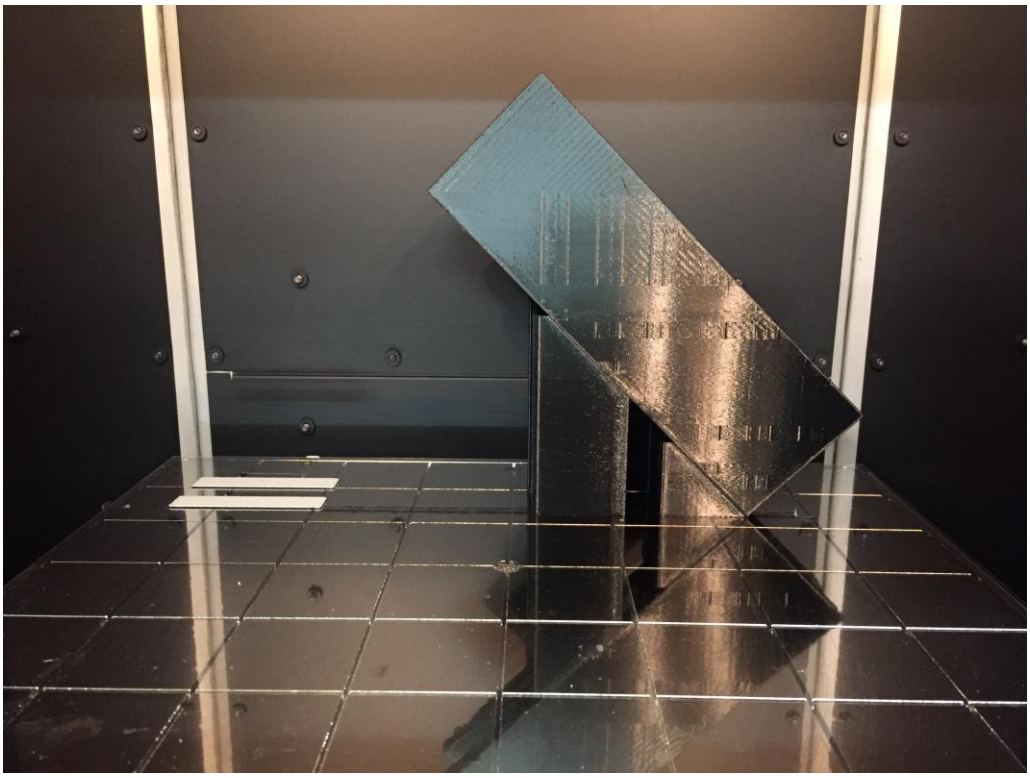

Figure A-5 3D Printed 45^0 Oriented Stiffened Scaled Plate Models at 45^0 Configuration

Figure A- 2 Bead 0^0 (left) and 45^0 (right) Orientation for 0^0 Configuration

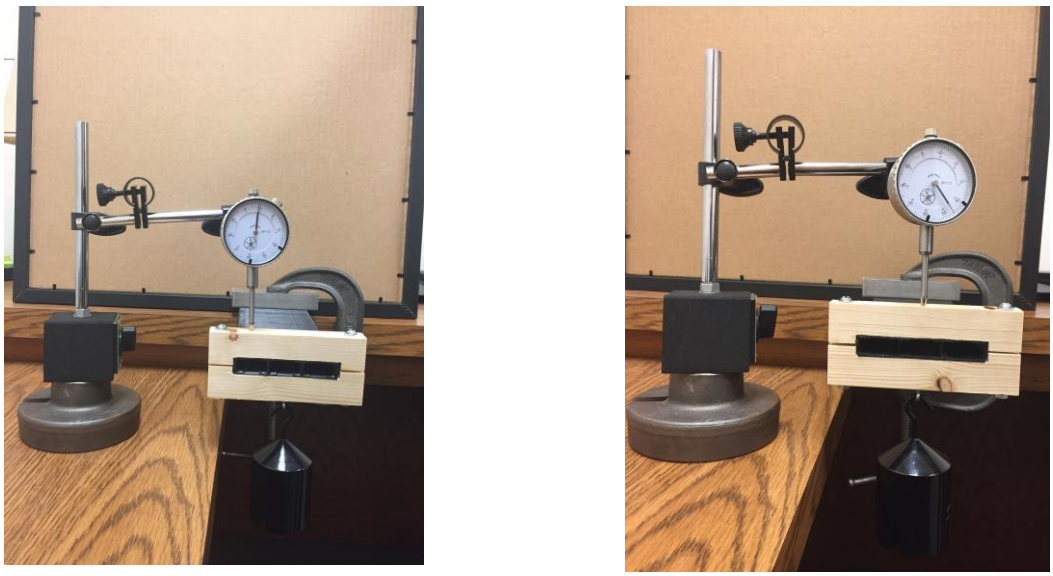

Figure A- 4 Bead 0^0 (left) and 45^0 (right) Orientation for 0^0 Configuration

Figure A- 2 Bead 0^0 (left) and 45^0 (right) Orientation for 45^0 Configuration

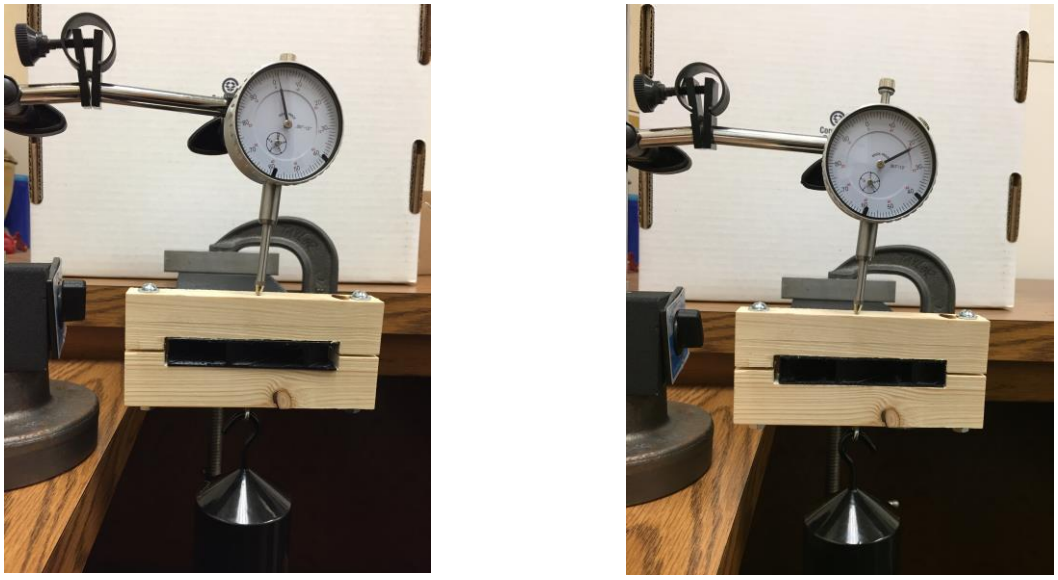

Figure A- 4 Bead 0 (left) and 45 (right) Orientation for 45^0 Configuration

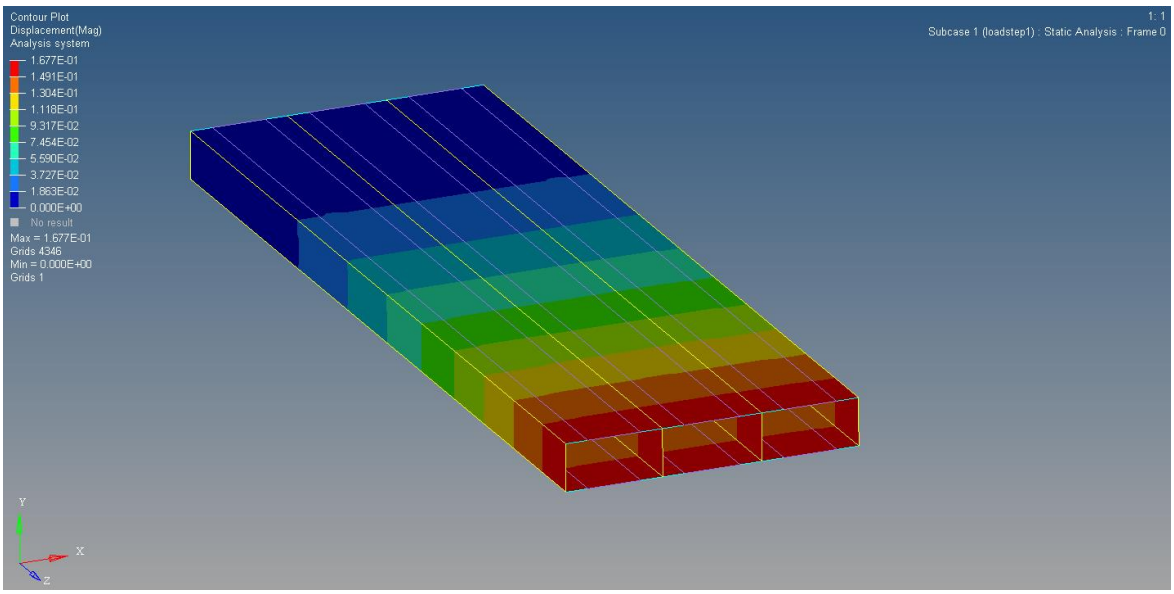

Figure A- 2 Bead 0^0 Configuration & 45^0 Orientation Cantilever Contour Plot

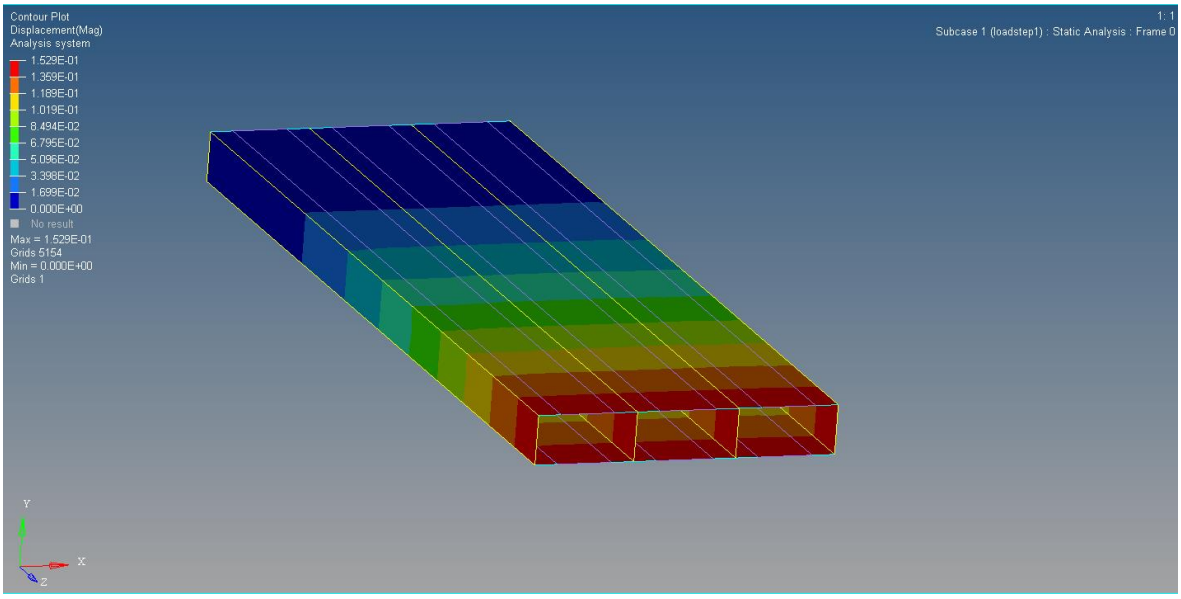

Figure A- 4 Bead 0^0 Configuration & 45^0 Orientation Cantilever Contour Plot

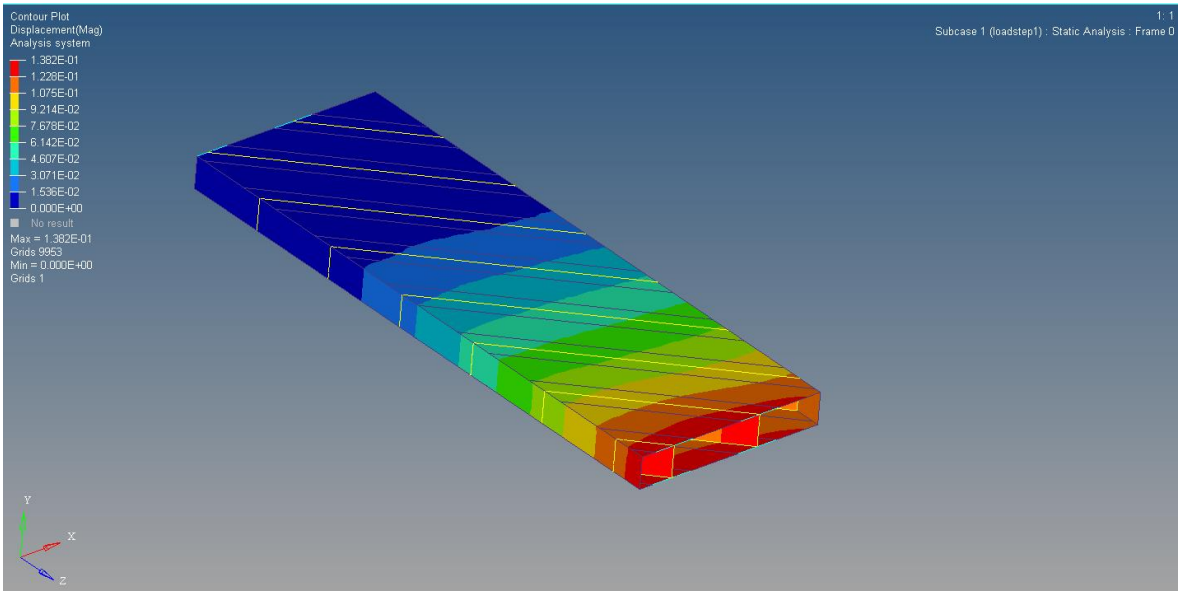

Figure A- 2 Bead 45^0 Configuration & 45^0 Orientation Cantilever Contour Plot

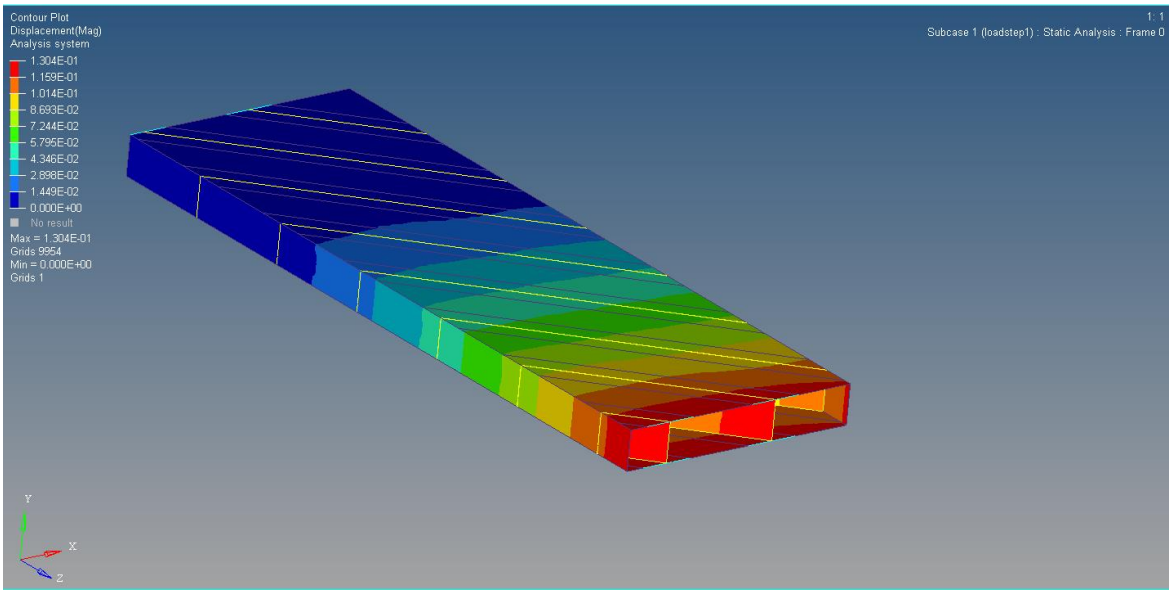

Figure A- 4 Bead 45^0 Configuration & 45^0 Orientation Cantilever Contour Plot

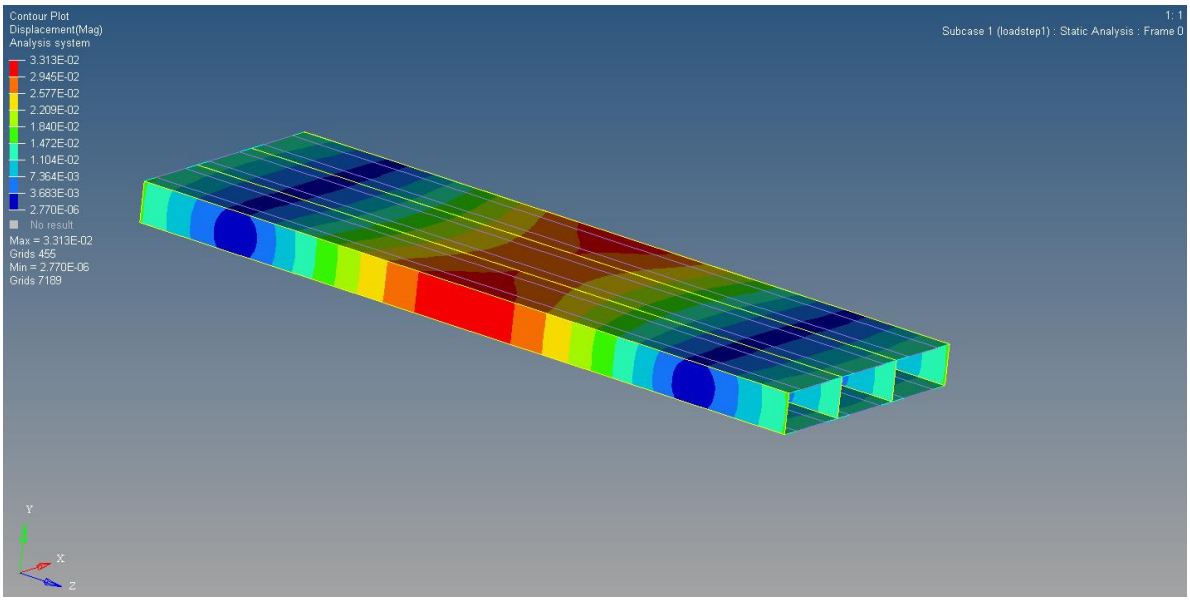

Figure A- 2 Bead 0^0 Configuration & 45^0 Orientation Three Point Bend Contour Plot

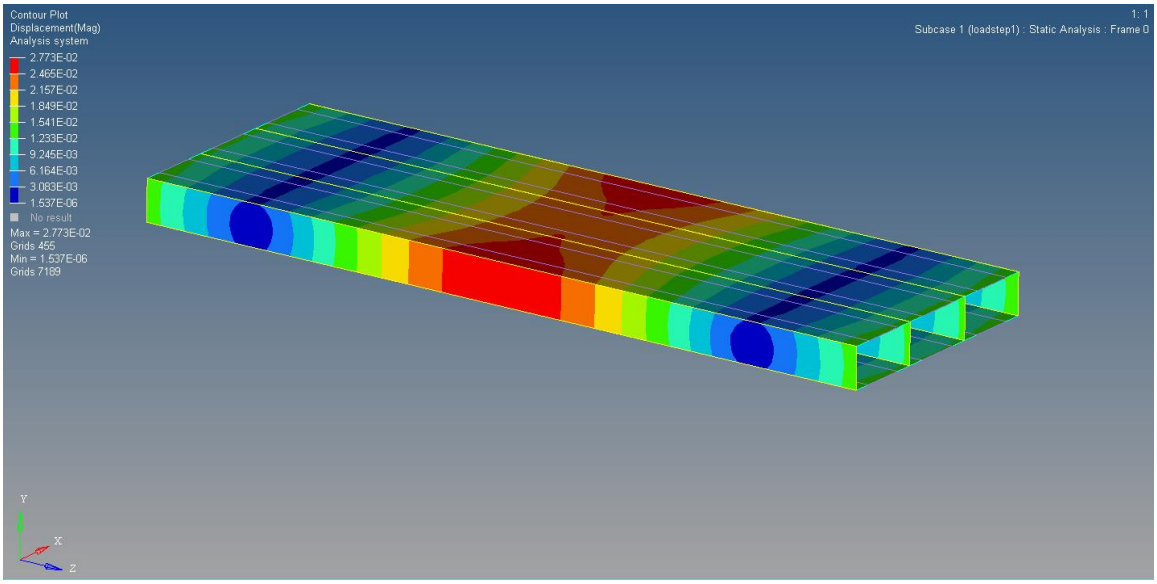

Figure A- 4 Bead 0^0 Configuration & 45^0 Orientation Three Point Bend Contour Plot

References

[1] Gibson, I., D. W. Rosen, and B. Stucker. *Additive Manufacturing Technologies: 3D Printing, Rapid Prototyping and Direct Digital Manufacturing*. Print.

[2] https://www.researchgate.net/figure/Schematic-of-fused-deposition-modeling-process-Source-18_fig1_324601411

[3] "Objet1000 Plus." *, Large 3D Printer*. Web

[4] Bisplinghoff, R., Ashley, H. and Halfman, R., *Aeroelasticity*, Addison-Wesley, Reading, Massachusetts, 1955.

[5] Shirk, M.H., Hertz, T.J., Weisshaar, T.A.., *Aeroelastic Tailoring—Theory, Practice, and Promise*, Journal of Aircraft., Vol 23, No 1, 6-18, 1986.\

[6] Wang, C., Yin, G, Zhang, Z, Wang, S, Zhao, T, Sun, Y., Yang, D., *Design and fabrication of an aircraft static aeroelastic model based on rapid prototyping*, Rapid Prototyping Journal, Vol 21, No 1, pp 34–42, 2015.

[7] Zhu W., Li D., Zhang Z., Ren K., Zhao X., Yang D., Zhang W., Sun Y., Tang Y., *Design and fabrication of stereolithography - based aeroelastic wing models*, Rapid Prototyping Journal, Vol. 17, No 4, pp.298-307, 2011.

[8] Heyes, A.L., and Smith, D.A.R., *Rapid Technique for Wind-Tunnel Model Manufacture*, Journal of Aircraft, Vol 42, No 2, pp 413-415, 2004.

[9] Chuk, R.N., and Thomson, V.J., *A comparison of rapid prototyping techniques used for wind tunnel model fabrication*, Rapid Prototyping Journal, Vol 4, No 4, pp. 185–196, 1998.

[10] Zhu, W, Zhao, X, Zhang, W, Ren, K, Zhang, Z, Li, D, *Design and Evaluation of Fully Configured Models Built by Additive Manufacturing*, AIAA Journal, Vol. 52, No. 7, 2014.

[11] Tyler, C., Braisted, W., and Higgins, J., *Evaluation of Rapid Prototyping Technologies for Use in Wind Tunnel Model Fabrication*, Proceedings of the 43rd AIAA Aerospace Sciences Meeting and Exhibit, Reno, Nevada, 2005.

[12] Lira, Sabine, Conklin, Lea, Taylor, *Design Optimization, Fabrication, and Testing of 3D Printed Aircraft Structure Using Fused Deposition Modeling*, SFF Symposium 2018

[13] Ziemian, C., Sharma, M., and Ziemian, S., *Anisotropic mechanical properties of ABS parts fabricated by fused deposition modelling,* Mechanical engineering. InTech, 2012.

[14] Ning, F., Cong, W., Qiu J., Wei J., and Wang S., *Additive manufacturing of carbon fiber reinforced thermoplastic composites using fused deposition modeling*, Composites Part B: Engineering 80 (2015): 369-378.

[15] Sweeney, C.B., Lackey, B.A., Pospisil, M.J., Achee, T.C., Hicks, V.K., Moran, A.G., Teipel, B.R., Saed, M.A. and Green, M.J., *Welding of 3D-printed Carbon Nanotube–polymer Composites by Locally Induced Microwave Heating*, Science Advances, Vol 3, No 6, 2017.

[16] P.M. Toal Jr, L.J. Holmes, R.X. Rodriguez, E.D. Wetzel, *Microstructured monofilament via thermal drawing of additively manufactured preforms*, Additive Manufacturing, Vol 16, pp 12–23, 2017.

[17] P. G. de Gennes, *Reputation of a Polymer Chain in the Presence of Fixed Obstacles*, The Journal of Chemical Physics, Vol 55, No 2, pp 572-579, 1971.

[18] Kim, Y., and Wool R., *A Theory of Healing at a Polymer-Polymer Interface*, Macromolecules, Vol 16, pp 1115-1120, 1983.

[19] Hart, K., and Wetzel E. *Fracture behavior of additively manufactured acrylonitrile butadiene styrene (ABS) materials*, Engineering Fracture Mechanics 177 (2017): 1-13.

[20] http://www.stratasys.com/-/media/files/material-spec-sheets/mss_fdm_absm30_1117a.pdf

Biographical Information

Edgar Bernardo Mares was born in Arlington, Texas. He received his high school diploma from Lamar High School in 2012. In 2016 he received his Bachelors of Science in Aerospace Engineering at the University of Texas at Arlington and in 2018 he received his Masters of Science in Mechanical Engineering from the same university.